

Beamforming for Mitigation of Interference for Different Antenna Array Geometry

by

KOMAL KUMARI

201915001

A Thesis Submitted in Partial Fulfilment of the Requirements for the Degree of

MASTER OF TECHNOLOGY

in

ELECTRONICS AND COMMUNICATIONS

with specialization in

Wireless Communication and Embedded Systems

To

DHIRUBHAI AMBANI INSTITUTE OF INFORMATION AND COMMUNICATION TECHNOLOGY

A program jointly offered with

C.R.RAO ADVANCED INSTITUTE OF MATHEMATICS, STATISTICS AND COMPUTER SCIENCE



July 2021

Declaration

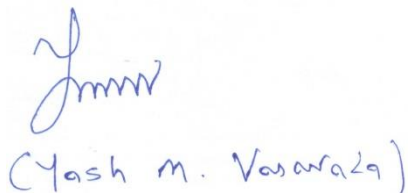
I at this moment declare that the Thesis comprises of my original work towards the degree of Master of Technology in Electronics and Communications at Dhirubhai Ambani Institute of Information and Communication Technology & C.R.Rao Advanced Institute of Applied Mathematics, Statistics and Computer Science, and has not been submitted elsewhere for a degree, due acknowledgment has been made in the text to all the reference material used. Due Acknowledgement has been made in the text to all the reference material used.

A handwritten signature in blue ink, reading 'Komal Kumari', is centered on the page. The signature is written in a cursive style.

KOMAL KUMARI

Certificate

This is to certify that the thesis work entitled has been carried out by Komal Kumari for the degree of Mater of Technology in Electronics and Communications at Dhirubhai Ambani Institute of Information and Communication Technology & C.R.Rao Advanced Institute of Applied Mathematics, Statistics and Computer Science under our supervision.



(Yash m. Vasavada)

Prof Yash Vasavada



Prof Sanjeev Gupta

Acknowledgments

Firstly, I would like to thank my supervisor Prof.. Yash Vasavada and Prof. Sanjeev Gupta for providing me with the opportunity to work under their supervision and continuous support and guidance throughout my work. Their invaluable expertise has nurtured me a lot during the process. I especially thank them for their unique ideas, directions and for always being available for discussion.

I would like to acknowledge my colleague members of CSPMI Laboratory for sparing out their precious time for all those quality discussions and feedbacks.

I am grateful to almighty for providing me with a healthy mind and the ability to do research work. I am also thankful to my family members, who had provided me with moral and emotional support throughout my career during this unprecedented time of the pandemic.

Table of Contents

List of Figures	9
Abstract.....	11
1 Introduction.....	15
1.1 General.....	15
1.2 The organization of the Thesis	18
2 Literature Review	19
2.1 Array Signal Model for Uniform Linear Array.....	19
2.2 ULA for single transmitter case	20
2.3 ULA for multiple transmitter case	21
3 Beamforming.....	23
3.1 The Mathematical model for conventional Beamforming	23
4 Beamforming simulations of ULA using MATLAB.....	30
4.1 Simulating the effect of changing the number of antennas for a single transmitting source.....	30
4.2 Simulation of the effect of changing the spacing between antennas	33
4.3 Beam Steering At Desired Angle	36
4.4 Simulation of Matched Filtering for multiple transmitters.....	39
5 Algorithms for Beamforming.....	41
5.1 Matched-filter (DFT) based power spectral density (PSD) estimation.....	41
5.2 Windowed-DFT based PSD estimator	42
6 Algorithms.....	44
6.1 Minimum Variance Distortion-less Response (MVDR) Method.....	44
6.2 Mathematical model	45

6.3	Simulation results.....	46
6.4	The MUSIC algorithm	48
6.5	Implementation steps	50
6.6	Simulation results.....	51
6.7	Expectation-Maximization Algorithm	53
6.8	Simulation result for Expectation Maximization.....	54
6.9	Comparative study of all algorithms.....	57
7	Uniform Planar Array	59
7.1	Array Factor of Uniform Planar Array.....	60
8	UNIFORM CIRCULAR ARRAY	66
8.1	MUSIC FOR UCA AND UPA	67
8.2	SIMULATIONS.....	71
9	Study Of Interference Cancellations Techniques.....	74
9.1	Least Square	75
9.2	MMSE solution	75
9.3	Block Diagram of Beamformer	77
9.4	Receiver performance Analysis.....	78
9.5	SIC(Successive Interference Cancellations)	79
9.6	PIC (Parallel Interference Cancellation).....	81
9.7	Interference Cancellation by Decision Feedback	83
9.8	Simulation Result	85
10	Conclusion and Scope of future work	87
10.1	Conclusion	87
10.2	Scope of Future Research.....	88
11	REFERENCES.....	90
12	Appendix.....	92

12.1	MATLAB CODES	92
------	--------------------	----

List of Figures

Figure 2-1 Illustrates of a plane wave incident on a uniformly spaced linear array from direction $\theta[2]$	20
Figure 3-1 Block Diagram for the schematic overview of Beamforming.....	23
Figure 3-2 Beamforming using weights.....	27
Figure 3-3 Plot for the linear array with different number of antennas.....	28
Figure 4-1 polar plot for M=1.....	31
Figure 4-2 polar plot for M=2.....	31
Figure 4-3 Polar plot for M=4.....	32
Figure 4-4 Pola Plot for M=10.....	32
Figure 4-5 Polar Plot for M=20.....	33
Figure 4-6 Polar plot for $d/\lambda = 0.1$	34
Figure 4-7 Polar plot for $d/\lambda = 0.3$	34
Figure 4-8 Polar plot for $d/\lambda = 0.5$	35
Figure 4-9 Polar plot for $d/\lambda = 0.7$	35
Figure 4-10 Polar plot for $d/\lambda = 0.9$	36
Figure 4-11 M=10 Beam-steering at -45 degree.....	37
Figure 4-12 M=10 Beam-steering at -30 degree.....	37
Figure 4-13 M=10 Beam-steering at -20 degree.....	38
Figure 4-14 M=10 Beam-steering at -10 degree.....	38
Figure 4-15 M=10 Beam-steering at 0 degree.....	38
Figure 4-16 M=10 Beam-steering at -45 degree.....	39
Figure 4-17 Match filer for multiple transmitter case.....	40
Figure 5-1 DFT based PSD estimation.....	42
Figure 6-1 MVDR PSD for theta [-20, 0 ,20].....	46
Figure 6-2 MVDR PSD for theta [0, 10 ,20].....	46
Figure 6-3MVDR PSD for theta [0, 15 ,20].....	47
Figure 6-4 MUSIC PSD simulation for theta [-20.0.20].....	51
Figure 6-5 MUSIC PSD simulation for theta [0.10.20].....	52
Figure 6-6 MUSIC PSD simulation for theta [0.15.20].....	52
Figure 6-7 EM PSD simulation for theta [-20,0,20].....	55
Figure 6-8 EM PSD simulation for theta [0,10,20].....	55

Figure 6-9 EM PSD simulation for theta [0,15,20]	56
Figure 6-10 MF vs MUSIC.....	57
Figure 6-11 PSD for all algorithms.....	58
Figure 6-12 PSD for all algorithms when theta=-30,0,5.....	58
Figure 7-1 Rectangular array	60
Figure 7-2 Array Factor of Uniform linear array for theta=30 and phi=45 for dx=dy=0.5	61
Figure 7-3 Array Factor of Uniform Planar array for theta=0 and phi=0 for dx=dy=0.562	
Figure 7-4 2-d Antenna radiation pattern for M=N=8 and theta= phi=0	63
Figure 7-5 3-d Antenna radiation pattern of isotropic elements for dx=dy=0.25 ,theta and phi=0.....	64
Figure 7-6 3-d Antenna radiation pattern of isotropic elements for dx=dy=1,theta=30 and phi=45	65
Figure 8-1 Uniform Circular Array.....	66
Figure 8-2 Polar Plot for N=8	67
Figure 8-3 Uniform Circular array.....	68
Figure 8-4 1-Dimensional MUSIC for UCA for DOA estimation of 30,60,120 degree	71
Figure 8-5 2-Dimensional MUSIC for UCA.....	72
Figure 8-6:1-Dimensional DOA estimation for UPA for MUSIC algorithm for 30,60,120	72
Figure 9-1 Block diagram for Beamformer	77
Figure 9-2 SIC.....	80
Figure 9-3 PIC	82
Figure 9-4 Plot for Avg. BER and number of User K.....	85
Figure 9-5 Plot for avg BER nad snr for user 1.....	85

Abstract

DOA estimation and Beamforming is one of the most crucial requirements of the Communication system design of RADAR, Satellite communication, Wireless communication. This Estimation performance differs for different antenna-array geometry. Remarkable progress in algorithm development has been made over the last decade. Using a sensor array of a particular configuration, we can improve the parameter estimation accuracy from the observation data in the presence of interference and noise. This Thesis is interested in how different algorithms for estimation perform for different antenna-array geometry and their comparative performance study. This motivates us to study interference and jamming attacks and comparative study on their performance. We will focus on conventional matched filter-based Beamforming, MVDR, MUSIC, and Expectation Maximization. We will review the version and limitations of these methods. A simulation model in MATLAB is used for the performance analysis. This thesis provides an overview of the conventional beamforming method, matched filtering method, MVDR, Expectation-Maximization, and the MUSIC method for DOA estimation and a study of their estimation error for ULA. We analyzed the planar array and circular array and MUSIC algorithm for both. We researched different interference cancellation techniques and performed their MATLAB comparative simulation study.

Keywords: *Beamforming, Planar Array, Linear Array, MUSIC, MVDR, Matched Filter*

List of Principal Symbols and Acronyms

M	Isotropic directional antenna elements
d	Element spacing
N	Uncorrelated narrow band sources
Θ_i	source arriving from the direction
K	Samples
$X(n)$	$KM \times$ Array output vector
$A(\theta)$	$NM \times$ Array steering matrix
$W(n)$	$KM \times$ Noise matrix
2σ	Noise covariance matrix
R_{xx}	Spatial correlation matrix
$[\cdot]_E$	Expectation

H	Complex conjugate transpose
E_S	N signal eigenvectors
E_N	Noise eigenvectors
$k\varphi$	Azimuth angle
$k\theta$	Elevation angle
X	$KN \times$ element space data matrix
A	$pN \times$ element space array manifold
e_i	Noise eigenvalues
E_S	N signal eigen vectors
E_N	Noise eigen vectors
P_{Music}	Angular spectrum
R	Circle with the radius

p

Equi-powered sources

Chapter-1

1 Introduction

1.1 General

In modern communication and radar applications, array antennas have become common. Array Signal Processing involves processing signals received by the antenna array, strengthening the message signals, mitigating the noise signals, and estimating signal parameters. Due to the inherent nature of an array antenna, incoming signals received at the antenna often undergo some form of spatial processing treatment in addition to the traditional temporal processing chain. By taking advantage of the duality in nature between time-frequency domain and spatial-frequency domain processing, many digital signal processing techniques like Fourier Transform and Finite Impulse Response Filtering techniques have been used to extract the desired information received signals. Angle of arrival (AOA) estimation is helpful in many applications such as positioning and signal enhancement.[1] Many estimators were developed in the literature to estimate the AOAs. These methods were initially designed to evaluate the AOAs in one plane. These methods utilized different antenna array structures. The most popular of these antenna array structures is the uniform linear antenna array (ULA). Due to relatively simple implementation, Uniform Linear Array (ULA) is a famous geometry for array signal processing.[2] Sensor Array Signal Processing has been essential for analyzing received data at the sensor end. Compared to traditional signal sensors, the sensor array can control the beam flexibility with a high signal gain and a solid ability to handle interference.[3] Hence, the sensor array

gives better resolution and performance in signal reception and parameter estimation. Thus, one of the essential uses of Array Signal Processing is the Direction of Arrival (DOA) estimation. It has various applications in wireless communication, sonar, tracking of objects, radio direction finding, etc. We discuss the problem of locating the signal sources using array sensors in this Thesis. This problem analyzes the energy distribution with source position representing the high concentration of energy in space. We discuss the model for the output signal of the receiving sensor array. The source location problem turns into a parameter estimation problem with such a model, under certain assumptions discussed later in this chapter. This parameter characterizes source locations in the direction of arrival(DOA). The direction of Arrival(DOA) estimation thus determines the angle of arrival of a spatially propagating signal at the receiver array.

The following assumptions are made for the Direction of Arrival Estimation in the Thesis.[4]

1. Point source- The signal source is taken as a point source. The direction from the antenna array can thus be estimated uniquely.
2. Narrowband signal- This is to ensure that all the array elements in the receiver can capture the signal at the same time
3. Array assumptions- The sources are assumed to be situated in the far-field of the array. The sources and the sensors in an array are believed to be in the same plane. Also, the propagation medium is assumed to be homogeneous so that the waves arriving at the array can be considered planar. Under these assumptions, the source location can be characterized using the direction of arrival (DOA) parameter.

The Smart antenna (multiple antennas, adaptive, or digital) is an antenna array. It uses intelligent signal processing algorithms for identifying the direction of arrival (DOA) of the signal. Based on DOA, it calculates the beamforming vector. The vector is used to locate and track the target. Beamforming is used to produce a focused signal

radiation pattern achieved by adding phases of signals in the desired direction based on variable traffic and signal surroundings. These techniques increase the signal power received by the user. Undesired or interfering signals like multipath interference, channel interference are null in the Beamforming technique. It increases the capacity of wireless communication. An antenna array consists of antenna elements that are spatially distributed at known locations regarding a common point. Changing the phase and amplitude of the exciting currents in each antenna element makes scanning the main beam electronically and placing nulls in any direction.[2]

The antenna elements can be arranged in various geometries, with standard linear, circular, and planar arrays. In the case of a linear array, the centers of the elements of the array are aligned along a straight line. If the spacing between the array elements is equal, it is called a uniformly spaced linear array. A circular array is one in which the centers of the array elements lie on a circle. In a planar array, the centers of the array elements lie on a single plane. Both the linear array and circular array are exceptional cases of the planar array. [5] In a smart antenna system, we use various algorithms to calculate the weights of smart antenna arrays to increase the output in the desired direction and reduce the power in an unwanted direction. We are using different types of arrays, i.e., linear array, circular array, planar array. We tried to implement a system model for ULA for single-user for our research purpose than for multiple users. Our planer and circular array research is still in progress[1].

However, this topology has some drawbacks. For example, the ULA is 1-D, and so it can estimate AOA estimation in one-dimensional applications; however, today's applications are interested in multi-dimensional (M-D) AOA estimation. Thus, planar arrays and 3-D arrays are needed to be exploited. Another drawback of the ULA is that it does not have uniform performance; the AOA estimation performance degrades considerably close to end-fire directions. This major drawback can be resolved by employing other array geometries[7]

1.2 The organization of the Thesis

This Thesis is organized as follows: Chapter 2 Literature Review. Chapter 3 Beamforming and the Model for the Uniform Planar array and its array factor Simulations. Chapter 4 is Beamforming of ULA using MATLAB. Chapter 5 will be consisting of Algorithms for Beamforming. Chapter 6 will be composed of advanced Algorithms. Chapter 7 consists of the Uniform Planar Array and Chapter 8 consisting Uniform Circular Array and its simulation, and Chapter 9 consists of the study of interference cancellation technique. The last section appendix will consist of all MATLAB codes.

Chapter 2

2 Literature Review

This chapter serves as an introduction to the direction of the arrival estimation problem. The signal model and modeling assumptions are presented, along with several commonly used DOA estimation algorithms.

2.1 Array Signal Model for Uniform Linear Array

We focus our discussion on a uniform linear array (ULA) with N elements, spaced equally at a distance d apart (usually chosen as the half-wavelength where the carrier's carrier wavelength is). The sensors are located at integer multiples of d . Hence, taking the first element as the origin, we can use the integer set $U = \{0, 1, \dots, N - 1\}$ to describe the sensor locations and geometry.

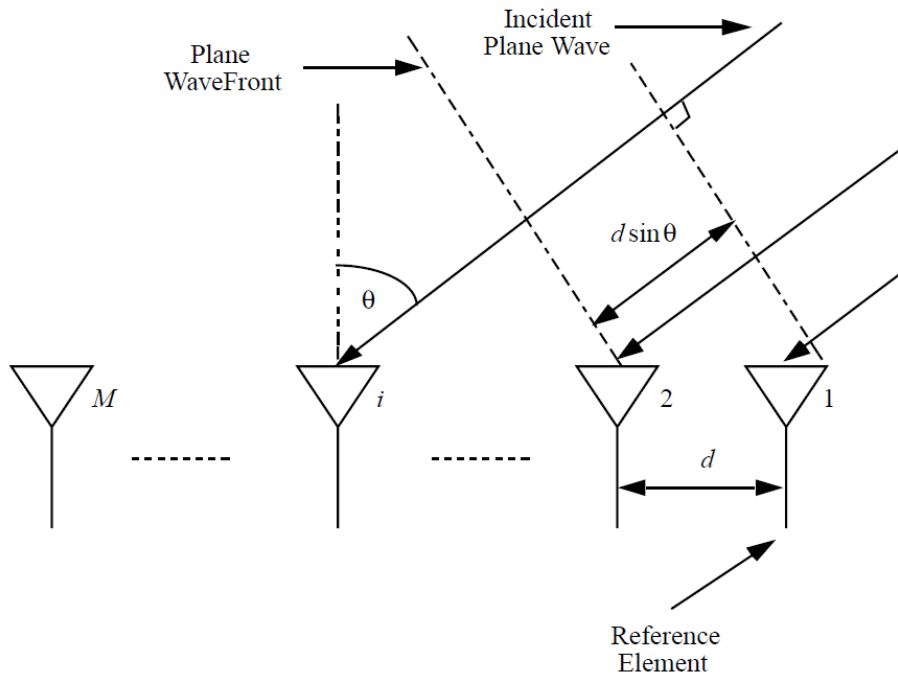


Figure 2-1 Illustrates a plane wave incident on a uniformly spaced linear array from direction θ [2].

The array elements are equally spaced by a distance d , and a plane wave arrives at the array from a direction θ the array broadside. The angle θ is called the direction-of-arrival (DOA) or angle-of-arrival (AOA) of the received signal and is measured clockwise from the broadside of the array.[2]

The wavefront corresponding to RF signal $x(t)=\exp(j2\pi ft)$ arrived at antenna making angle θ with vertical at the antenna. The wavefront takes a constant time τ to reach the next element from the previous one.

2.2 ULA for single transmitter case

- A signal received at first element: $(t) = \exp(j2\pi ft)$
- The time delay between adjacent elements = $d\sin\theta/c$.
- Signal received at kth element= $\exp(j2\pi f(t - k - 1))\tau$

$$x_k(t)=\exp(j2\pi ft) * \exp(j2\pi f(k - 1) * \tau) \quad (1)$$

$$X(t) = \begin{bmatrix} x_1(t) \\ x_2(t) \\ x_3(t) \\ \vdots \\ \vdots \\ \vdots \\ x_M(t) \end{bmatrix} \quad (2)$$

$$a(\theta) = \begin{bmatrix} 1 \\ \exp(-j2\pi f\tau) \\ \exp(-j(2)2\pi f\tau) \\ \exp(-j(3)2\pi f\tau) \\ \vdots \\ \vdots \\ \exp(-j(M-2)2\pi f\tau) \\ \exp(-j(M-1)2\pi f\tau) \end{bmatrix} \quad (3)$$

$a(\theta)$ is the steering vector.

$X(t)$ referred to as the array input data vector or the illumination vector

$$X(t) = a(\theta) \times x_1(t) \quad (4)$$

$f_s \geq 2f_m$ (Nyquist sampling theorem), f_s =sampling frequency f_m =maximum analog frequency in the time domain. In the space domain, $f_s = \lambda/d$ is sampling frequency $f_m = 1$ (because $\sin(\theta) \leq 1$) and $\sin(\theta)$ analogous to spatial frequency, therefore, $d \leq \lambda/2$ and optimum distance between antennas should be $\lambda/2$

2.3 ULA for multiple transmitter case

Suppose there are q narrowband signals all centered around a known frequency, say f , impinging on the array with a DOA $\theta_i(t)$ for $i=1,2,\dots,q$. These signals may be uncorrelated, as for the signals coming from different users. The received signal at the

array is a superposition of all the impinging and noise. Therefore, the input data vector may be expressed as

$$X(t) = \sum_{i=1}^q a(\theta_i) s_i(t) + n(t) \quad (5)$$

$A(\Theta)$ is the $M \times q$ matrix of the steering vectors and in matrix form

$X(n) = A(\Theta) s_i(n) + n(n)$ for n samples of data

$$A(\Theta) = \begin{bmatrix} 1 \\ \exp(-jk d \sin \theta_i) \\ \exp(-j(2)k d \sin \theta_i) \\ \exp(-j(3)k d \sin \theta_i) \\ \vdots \\ \vdots \\ \vdots \\ \exp(-j(M-2)k d \sin \theta_i) \\ \exp(-j(M-1)k d \sin \theta_i) \end{bmatrix} \quad (6)$$

Where $k = 2\pi / \lambda$

Chapter 3

3 Beamforming

The main goal of sensor array signal processing is to estimate parameters and extraction of information by fusing temporal and spatial data captured via sampling a wavefield with a set of judiciously placed sensors.

Beamforming is the signal of interest that comes from only one particular direction and impinges different sensors at the receiver. The resultant signal gives a higher strength because of coherent combining. Coherent combining is done after proper phase compensation at each sensor. Thus, the resulting gain of the sensor would look like a sizeable dumb-bell-shaped lobe aimed in the direction of interest. This critical concept is used in different communication, voice, sonar applications[2].

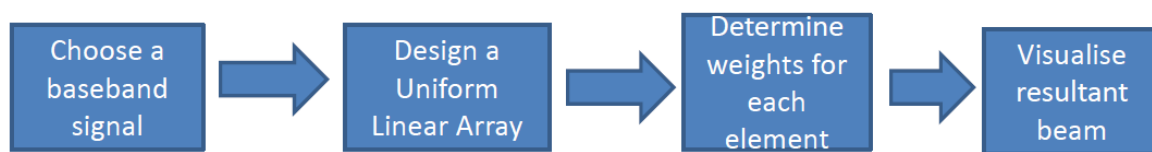


Figure 3-1 Block Diagram for the schematic overview of Beamforming

3.1 The Mathematical model for conventional Beamforming

The conventional beamforming method for finding DOA uses the basics of spatial filtering. An array of sensors are used here as receivers as they can be steered

electronically instead of the mechanical complications in a fixed antenna. Weighing factor operation is done to linearly combine the sensor output and get a single output signal $y(n)$ [3].

$$y(n) = w^H x(n) \quad (7)$$

Where superscript H denotes the Hermitian operation, and the response of this spatial filter can be described by its effective antenna pattern $P(\theta)$.

$$P(\theta) = |w^H a(\theta)|^2 \quad (8)$$

$P(\theta)$ is the average power of the response from the spatial filter when the unity power signal arrives from angle θ . The gains and phases in w create proper beams and nulls. The effective array patterns are quite different from the individual components. It could be seen that the gain of individual sensors would be just a horizontal line when plotted as a function of the DOA of the signal. The total average power in the output can thus be expressed as P_{total} where

$$P_{total} = \langle |y(n)|^2 \rangle_N \quad (9)$$

Or
$$P_{total} = w^H R_{xx} w \quad (10)$$

where $\langle \cdot \rangle_N$ is the time averaging over N time samples, and R_{xx} is the spatial auto-correlation matrix of the data in the equation. This matrix contains information about the array response vectors.

$$R_{xx} = \langle x(n)x(n)^H \rangle_N \quad (11)$$

$$R_{xx} = \langle (A(\theta) s_i(n) + n(n)) \times (A(\theta) s_i(n) + n(n))^H \rangle_N \quad (12)$$

$$\text{Therefore} \quad R_{xx} = A(\theta)R_{xx}A(\theta)^H + R_{ii} \quad \text{for} \quad (13)$$

$$N \rightarrow \infty$$

In Beamforming, angular sections of the region are scanned using the basic narrowband signal model. The weight w_b co-ordinates the phases on the incoming signal say coming from θ_0 . When vector $w_b = a(\theta_0)$ the antenna pattern will have the maximum gain from the direction from θ_0 . This happens because the weighing factor will add things constructively and give the required amplitude. This comes from Cauchy-Schwarz inequality:

The equality holds correct if and only if w is proportional to $a(\theta_0)$ for all vectors w . So the effective pattern beam pattern will have a global maximum at θ_0 In the absence of a rank-1 ambiguity. The direction of arrival angles is decided based on the local maxima of the received power. So basically, the beam monitors a region for each θ the average power $P_b(\theta)$ of the steered array is measured,

$$P_b(\theta) = \langle |y(n)|^2 \rangle_N \quad (14)$$

$$P_b(\theta) = \langle |w_b^H x(n)|^2 \rangle_N \quad (15)$$

$$P_b(\theta) = w_b^H R_{xx} w_b \quad (16)$$

$$P_b(\theta) = a(\theta)^H R_{xx} a(\theta) \quad (17)$$

R_{xx} would be the same for the data, reducing the computations for different regions under consideration. This helps to reduce the blind spots for detecting transient signals[4].

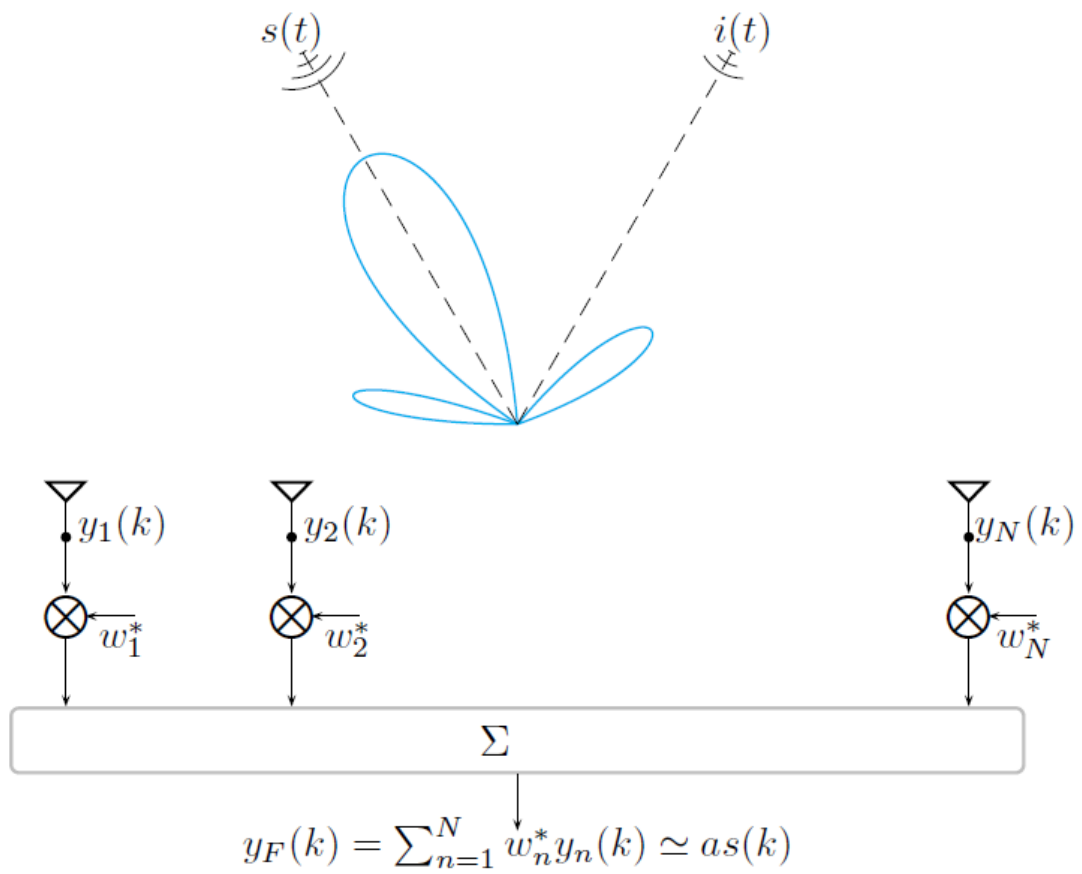


Figure 3-2 Beamforming using weights

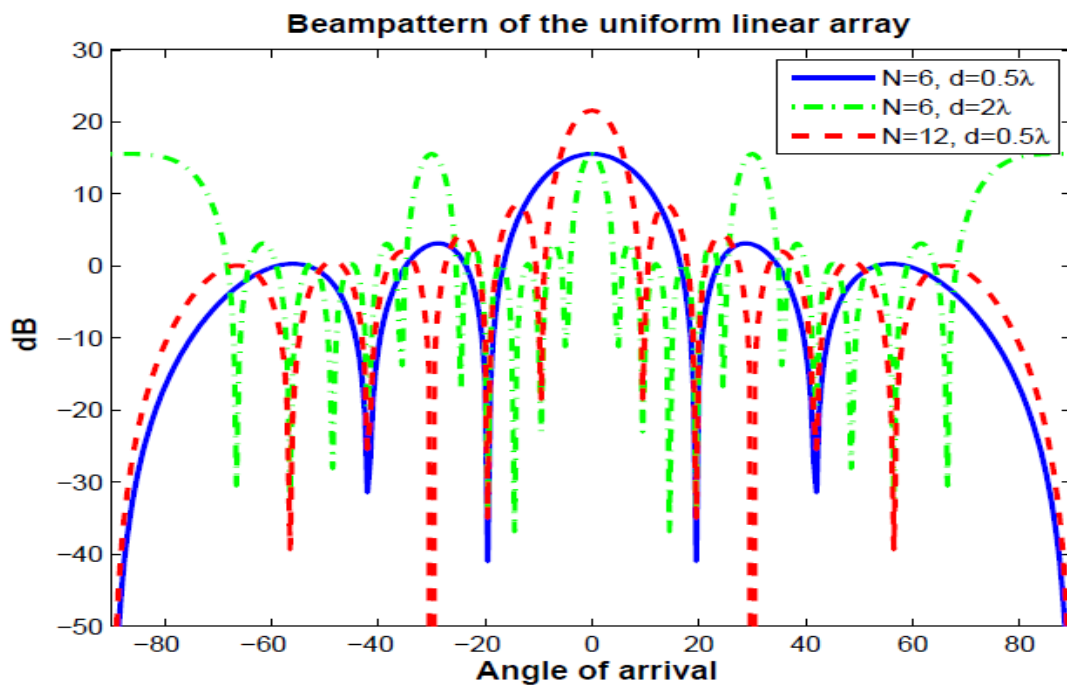


Figure 3-3 Plot for the linear array with different numbers of antennas

Adaptive Beamforming is a technique in which an array of antennas is exploited to achieve maximum reception in a specified direction by estimating the signal arrival from the desired direction. In contrast, signals of the same frequency from other directions are rejected. This process is achieved by varying the weights of each sensor used in the array. This allows the antenna system to focus the maxima of the antenna pattern towards the desired mobile while minimizing the impact of noise, interference, and other effects from undesired mobiles. The adaptive beamforming algorithms are categorized under two types according to whether a training signal is used or not. One type of these algorithms is the non-blind algorithm, in which a training signal is used to adjust the array weight vector. Another type is a blind adaptive algorithm which does not require a training signal. Spatially propagating signals encounter the presence of interfering signals and noise signals. If the desired signal and the interferers occupy the same temporal frequency band, then temporal filtering cannot separate the signal from the interferers. However, the expected and the interfering signals generally originate from different spatial locations. This spatial separation can be exploited to separate the signals from the interference. The purpose of DOA estimation is to use the data received by the array to estimate the direction of arrival of the signal. The variety then uses the results of DOA estimation to design the adaptive Beamformer, which maximizes the power radiated towards users and suppresses interference.

As a result, we can infer that a successful design of an adaptive array depends highly on the performance of the DOA algorithm. The direction of arrival algorithms is usually complex. Their performance depends on many parameters, such as the number of mobile users and the spatial distribution, array elements and their spacing, and signal samples. Several algorithms have been developed to determine the direction of arrival from the measurements of the signals received at the elements of array sensors. One of the simplest and popular algorithms used for DOA estimation is the MUSIC (MUltiple SIgnal Classification). The MUSIC algorithm is a subspace algorithm aimed at eliminating noise. This can be done by splitting the M -dimensional space spanned by the antenna element outputs into a signal subspace and a noise subspace

Chapter 4

4 Beamforming simulations of ULA using MATLAB

The output of Beamformer in the simplest case can be given by:

$$y(k) = \sum_{i=1}^k w_i^H x(k) \quad (18)$$

$$Y = w_i^H x(k) \text{ (Matched Filtering)} \quad (19)$$

$$\text{Where } w = \begin{bmatrix} 1 \\ \exp(-j2\pi f\tau) \\ \exp(-j(2)2\pi f\tau) \\ \exp(-j(3)2\pi f\tau) \\ \vdots \\ \vdots \\ \vdots \\ \exp(-j(M-2)2\pi f\tau) \\ \exp(-j(M-1)2\pi f\tau) \end{bmatrix} \quad (20)$$

This 'w' is the optimum weight when there is one source of interest.

4.1 Simulating the effect of changing the number of antennas for a single transmitting source.

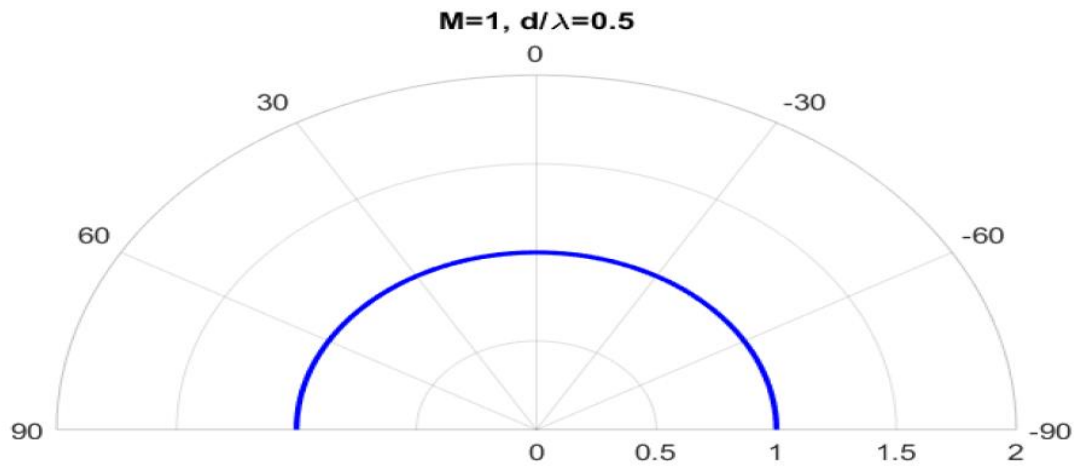


Figure 4-1 polar plot for M=1

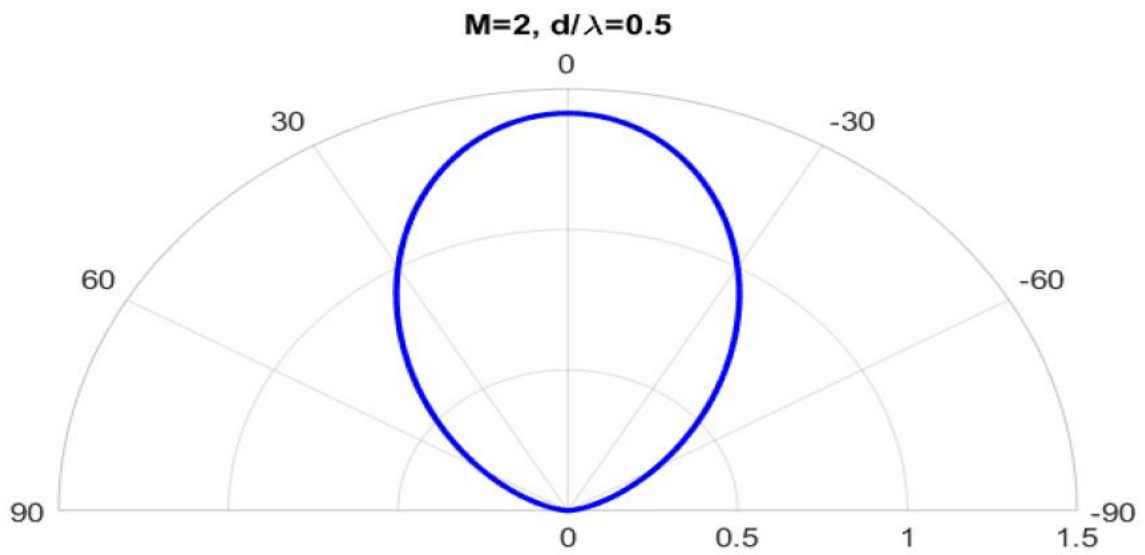


Figure 4-2 polar plot for M=2

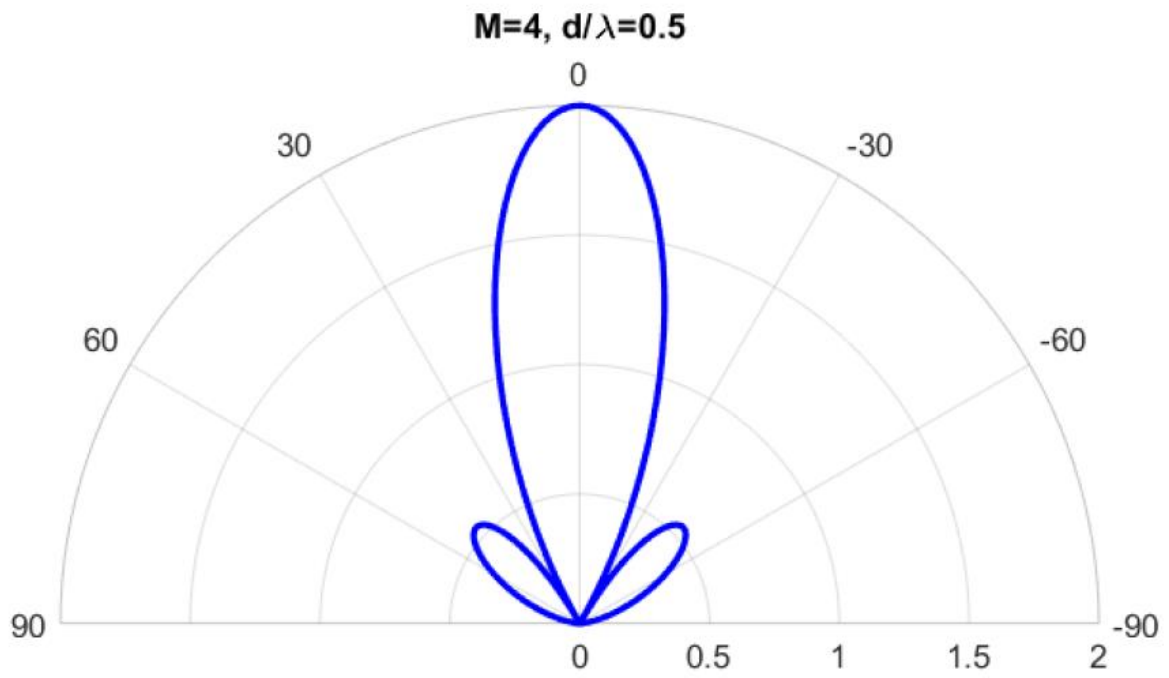


Figure 4-3 Polar plot for M=4

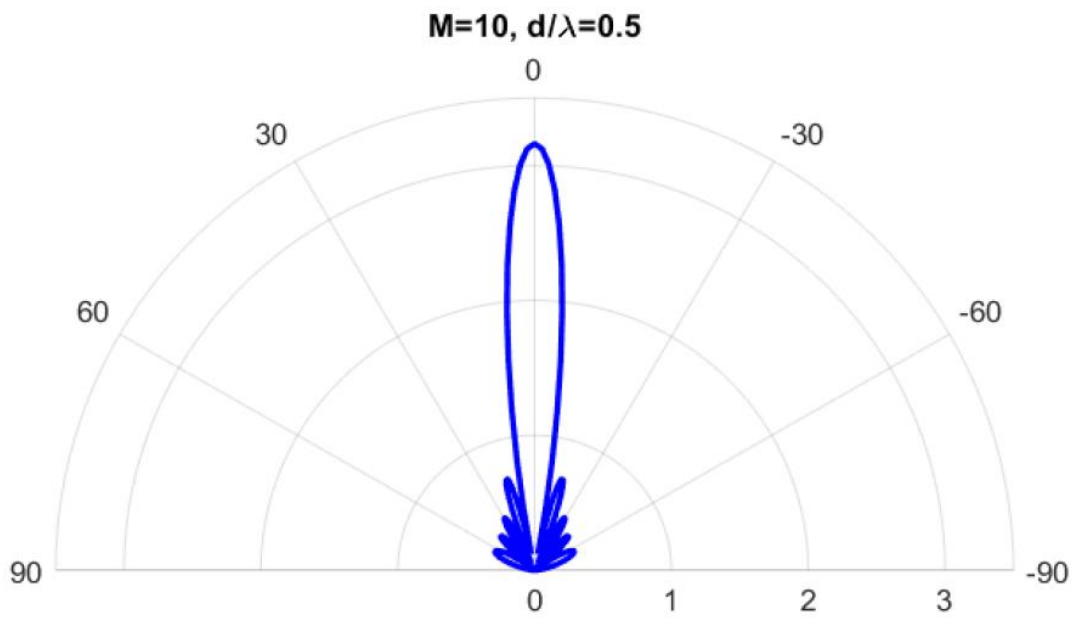


Figure 4-4 Pola Plot for M=10

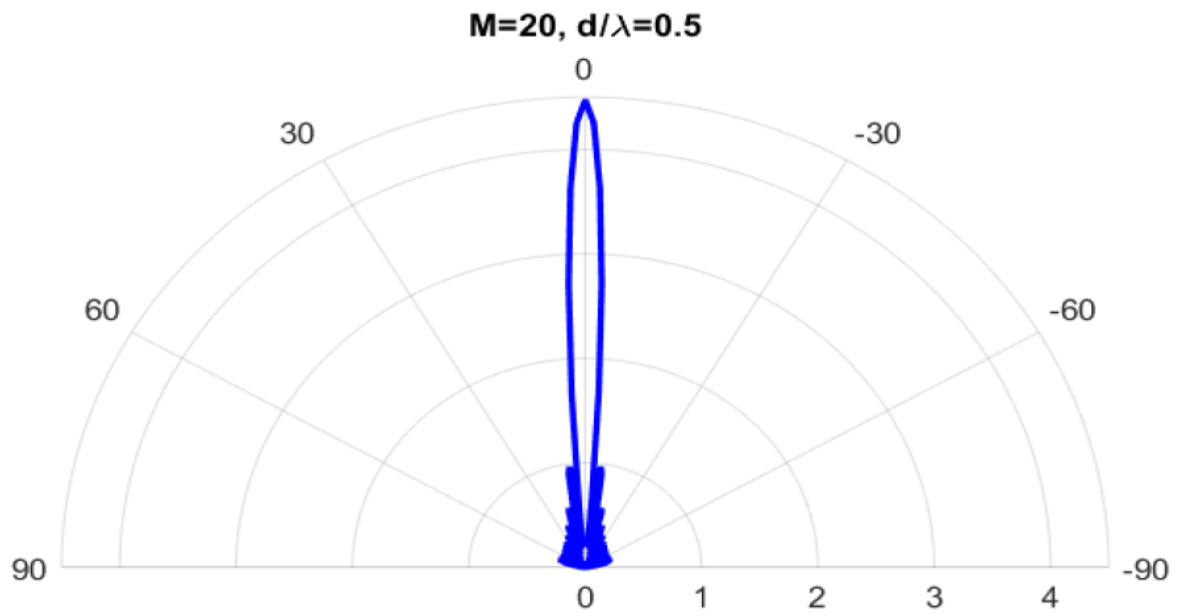


Figure 4-5 Polar Plot for M=20

It can be evident from the simulations that increasing the number of antenna elements gives a sharper beam.

4.2 Simulation of the effect of changing the spacing between antennas

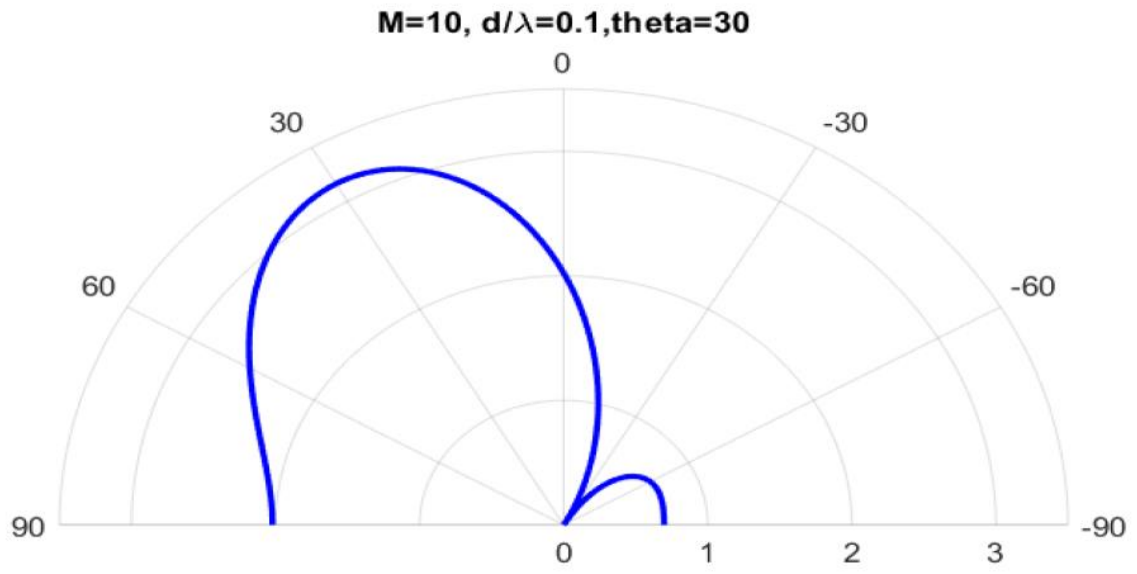


Figure 4-6 Polar plot for $d/\lambda = 0.1$

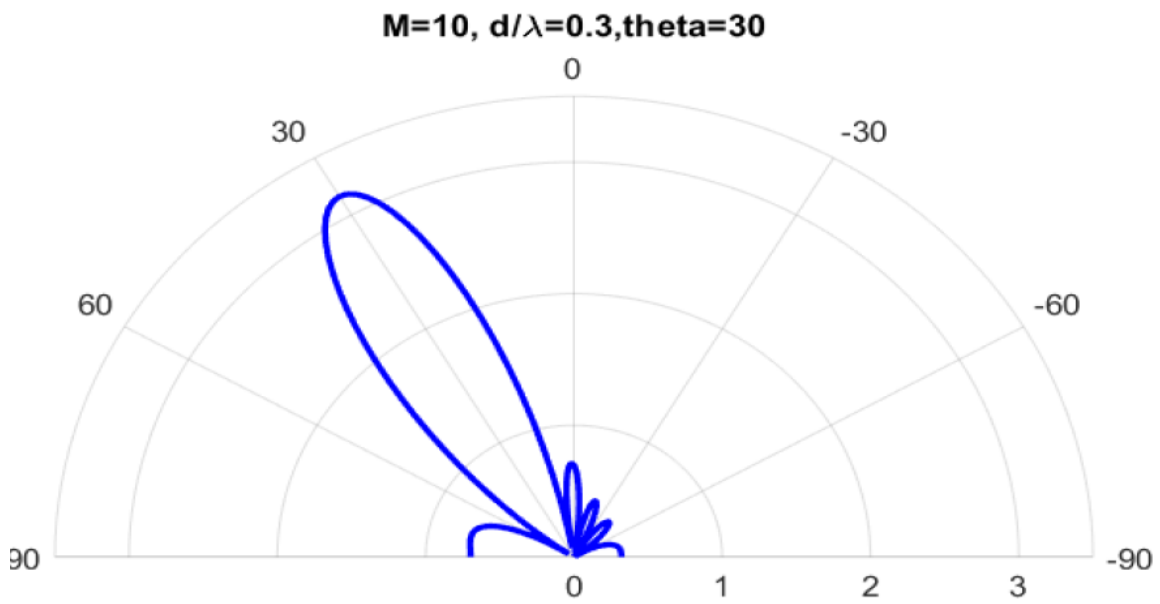


Figure 4-7 Polar plot for $d/\lambda = 0.3$

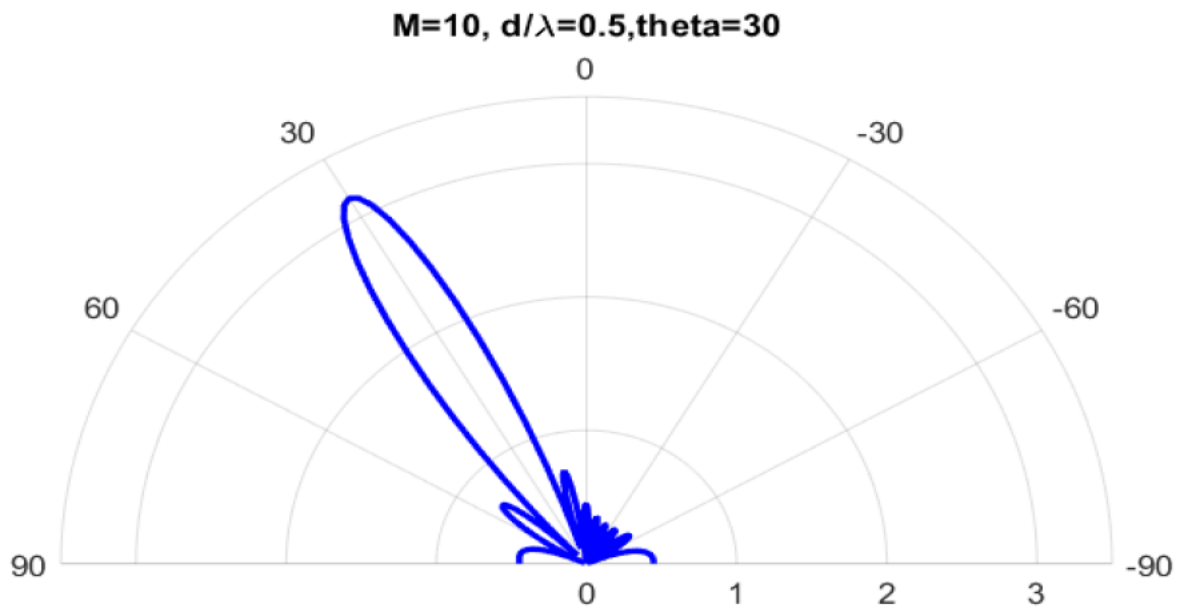


Figure 4-8 Polar plot for $d/\lambda = 0.5$

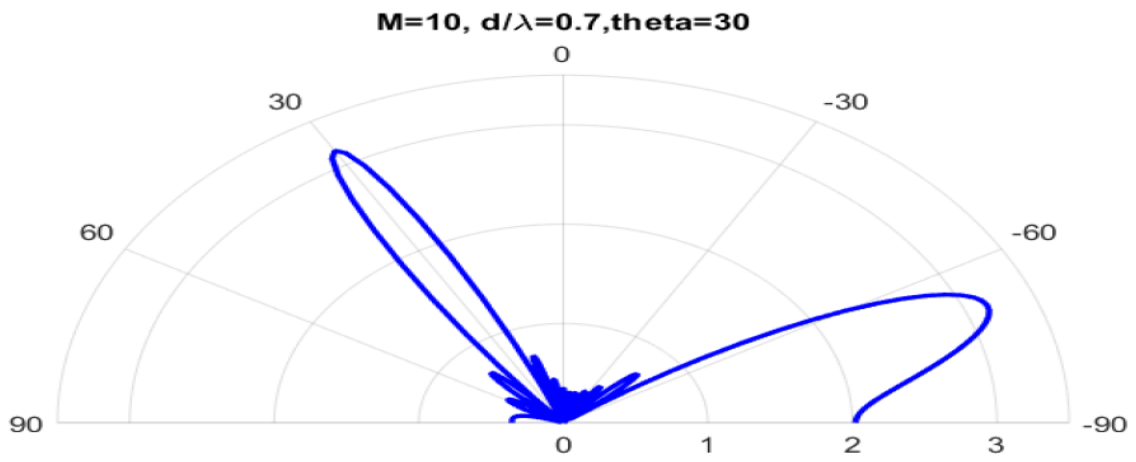


Figure 4-9 Polar plot for $d/\lambda = 0.7$

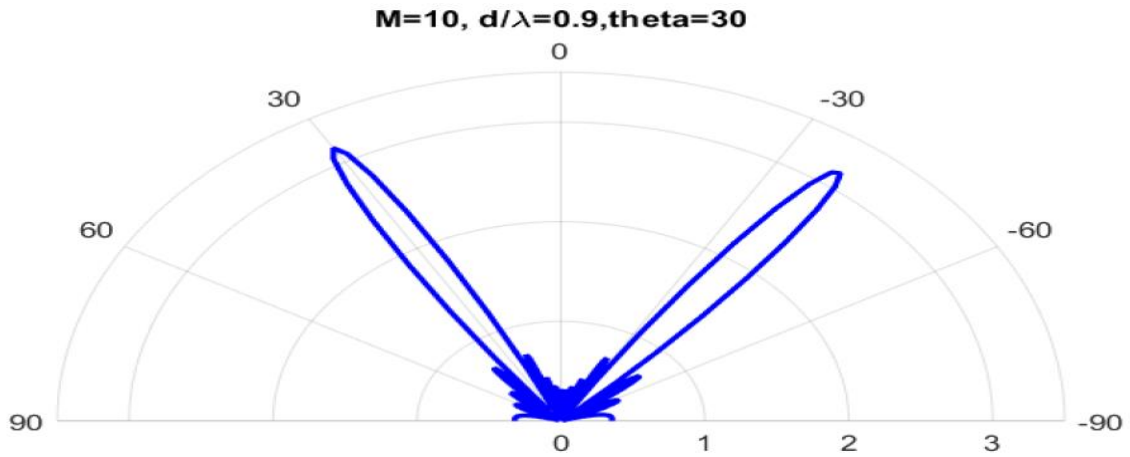


Figure 4-10 Polar plot for $d/\lambda = 0.9$

It is evident from the simulations that an increase in element spacing $d > (\lambda/2)$ leads to spatial aliasing. However, if the element spacing is decreased $d < (\lambda/2)$ the beam becomes wider. The optimal distance between each antenna is $\lambda/2$.

4.3 Beam Steering At Desired Angle

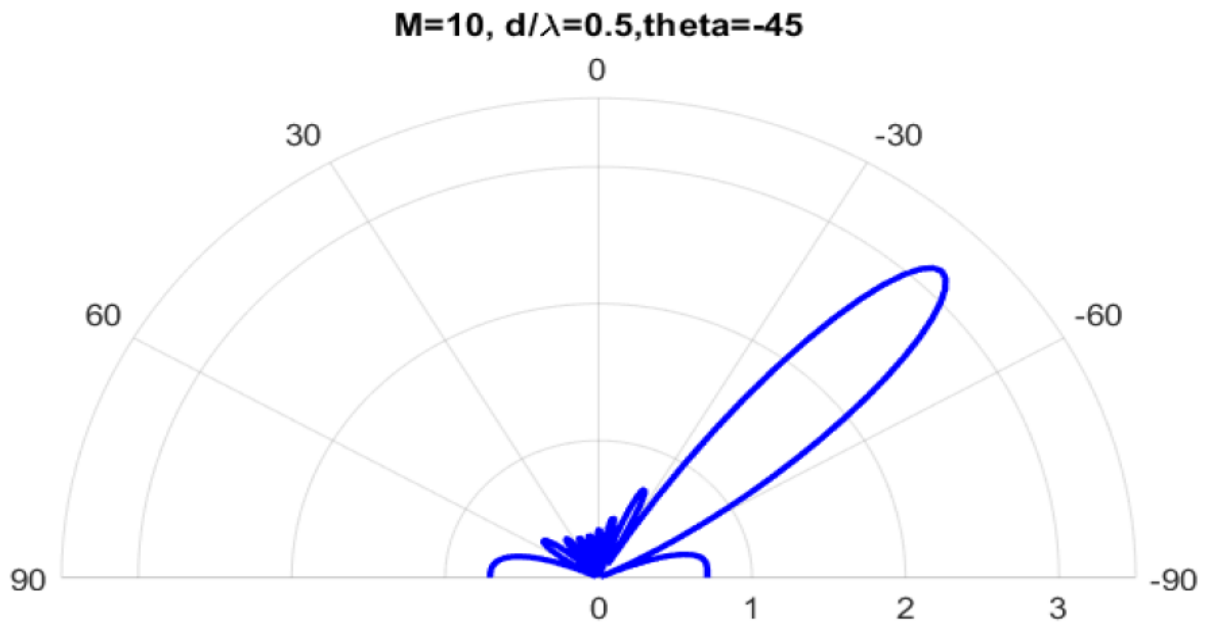


Figure 4-11 M=10 Beam-steering at -45 degree

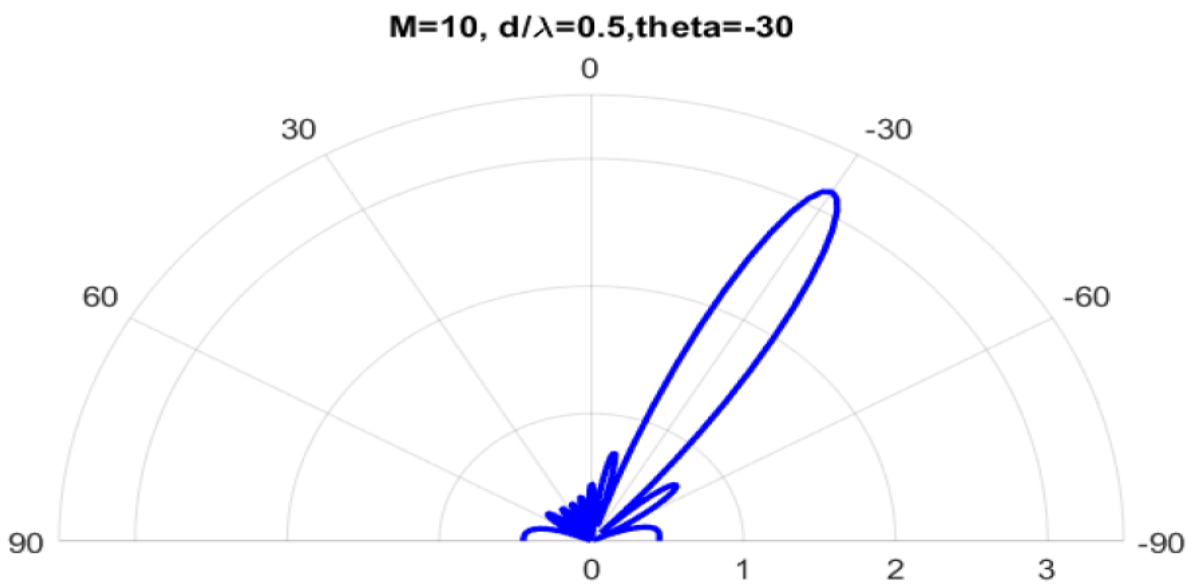


Figure 4-12 M=10 Beam-steering at -30 degree

Figure 4-13 M=10 Beam-steering at -20 degree

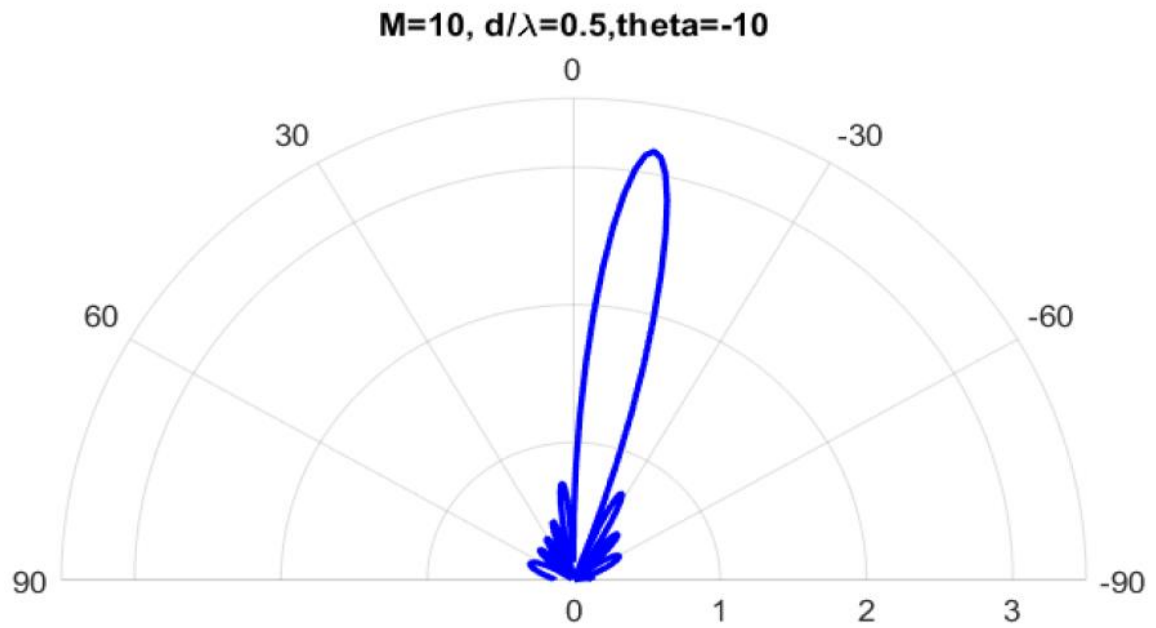


Figure 4-14 M=10 Beam-steering at -10 degree

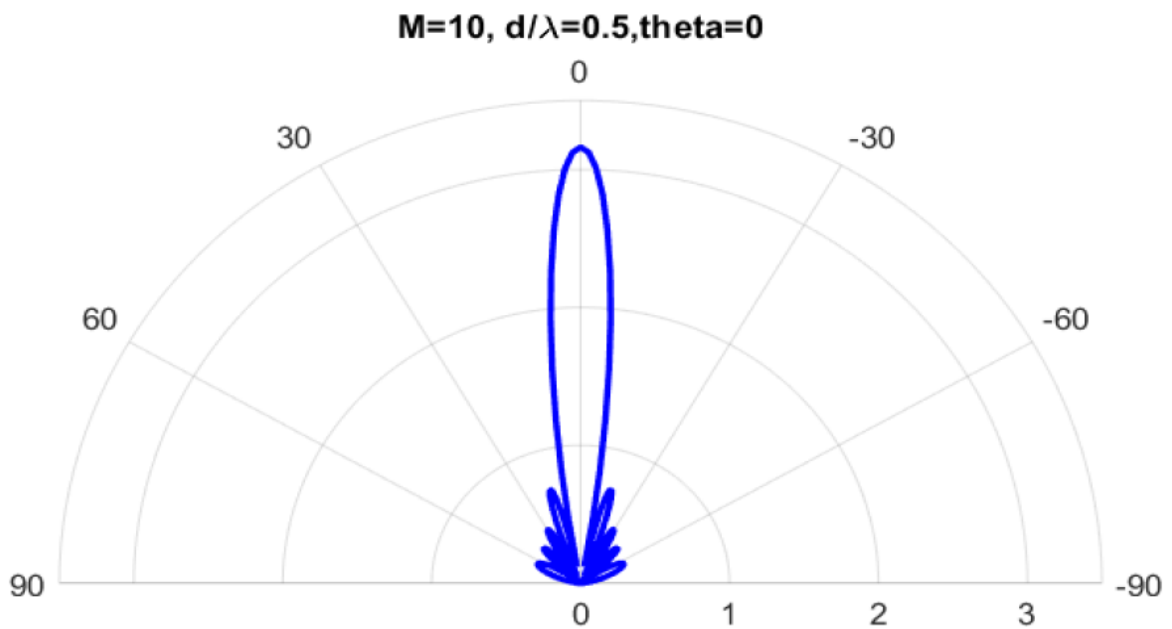


Figure 4-15 M=10 Beam-steering at 0 degree

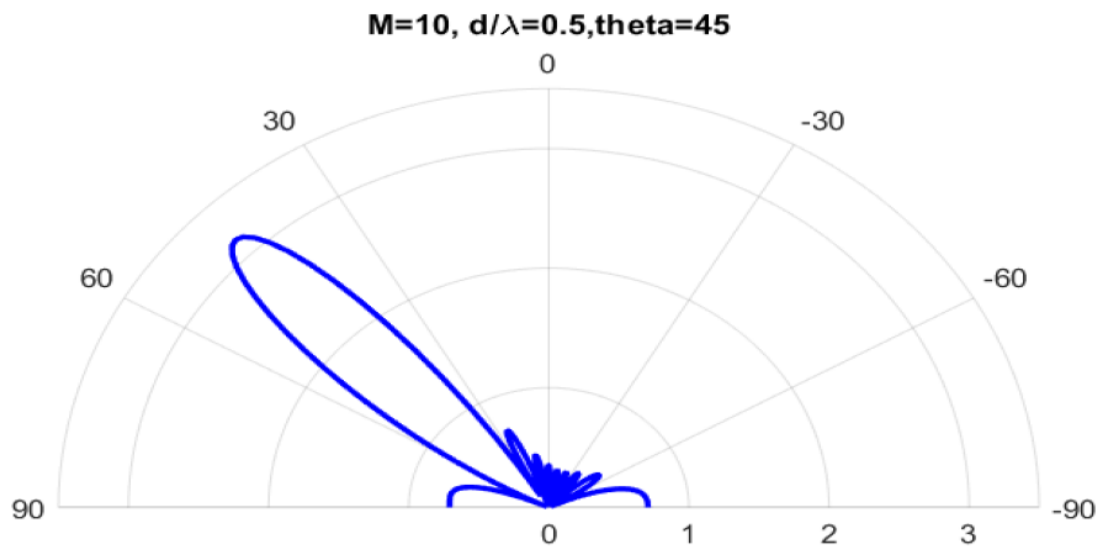


Figure 4-16 M=10 Beam-steering at -45 degree

The beam can be formed at any desired angle. Given an angle, the beam can be steered to another desired angle. Thus Beamforming gives us freedom of steering of beams at any desired angle.

4.4 Simulation of Matched Filtering for multiple transmitters

We keep our desired signal at 0 degrees and a set of interferers at 10,20, 30, 45, 60,75 degrees. This will be our simulation Testbed

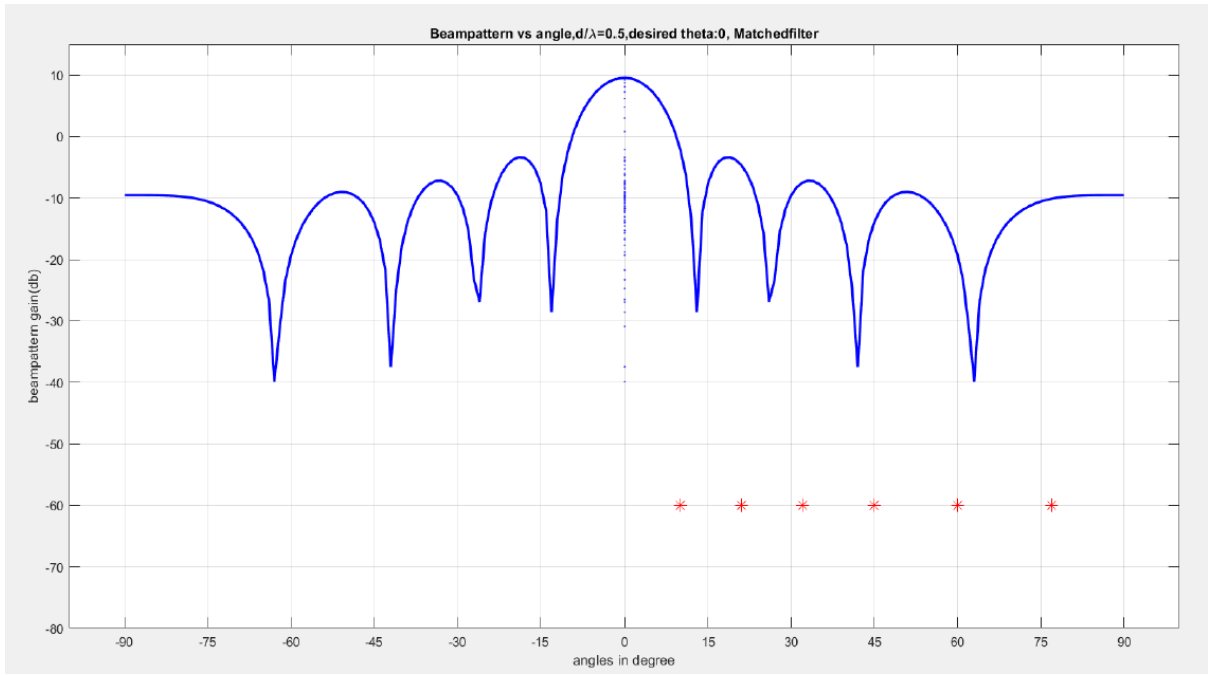


Figure 4-17 Match filter for multiple transmitter case

Chapter 5

5 Algorithms for Beamforming

5.1 Matched-filter (DFT) based power spectral density (PSD) estimation

Weighing factor operation is done to linearly combine the sensor output and get beamformer output signal $y(n)$.

$$y_n = w^H x_n \quad (21)$$

Where superscript H denotes the Hermitian operation, and the response of this spatial filter can be described by its effective antenna pattern $P(\theta)$.

$$P(\theta) = |w^H a(\theta)|^2 \quad (22)$$

$P(\theta)$ is the average power of the response from the spatial filter when the unity power signal arrives from angle θ . $E[|y_n|^2]$ evaluated using the filters w for different values of θ collectively provide the Power Spectral Density (PSD) of x_n

$$E[|y_n|^2] = w^H R_{xx} w \quad (23)$$

Wiener-Khinchine Theorem (WKT): The PSD and the ACF (autocorrelation function) of a random variable are Fourier Transform pairs. Using different w filters and taking that θ as being present for which $E[|y_n|^2]$ is the highest. These w_N^f filters, if $f = \frac{k}{N}$ and $k = 0, \dots, N - 1$, $f = \sin(\theta) / 2$, collectively define the columns of the DFT matrix. Alternatively, different columns of the DFT matrix, i.e., the filters $\{w_N^f\}$, can be viewed as Band Pass Filters (BPFs) centered at N equispaced frequencies from 0 to $\frac{N-1}{N}$. In the DFT operation, the input signal x_n is simultaneously (in parallel) passed through this set of BPFs and these BPS outputs $\{y_n\}$ collectively form the DFT of x_n . A

computationally efficient implementation of the DFT, i.e., the FFT, allows a fast computation of the outputs $\{y_n\}$. The expectation operation is implemented by averaging the set of $\{|y_n|^2\}$ over multiple observation vectors $\{x_n\}$. Thus, the process described earlier is an FFT-based method of estimating the PSD. A filter w_N^f is *matched* to the input signal x_n . It oscillates at frequency f . By the "matched filter," we mean that the FIR filter impulse response is identical to the input signal. The angle θ between the two vectors becomes zero, and the inequality turns into equality. For our simulation θ -reference= $[-20 \ 0 \ 20]$ and frequency of reference, $f_{ref}=\sin(\theta)/2$

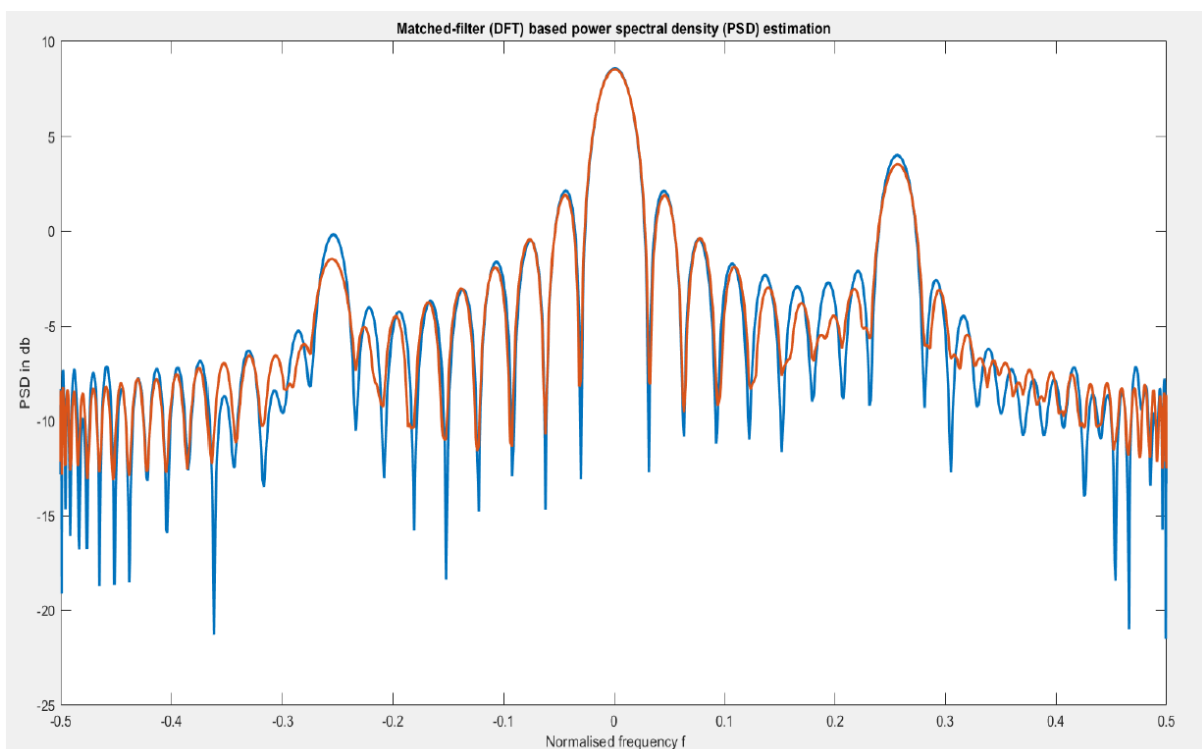
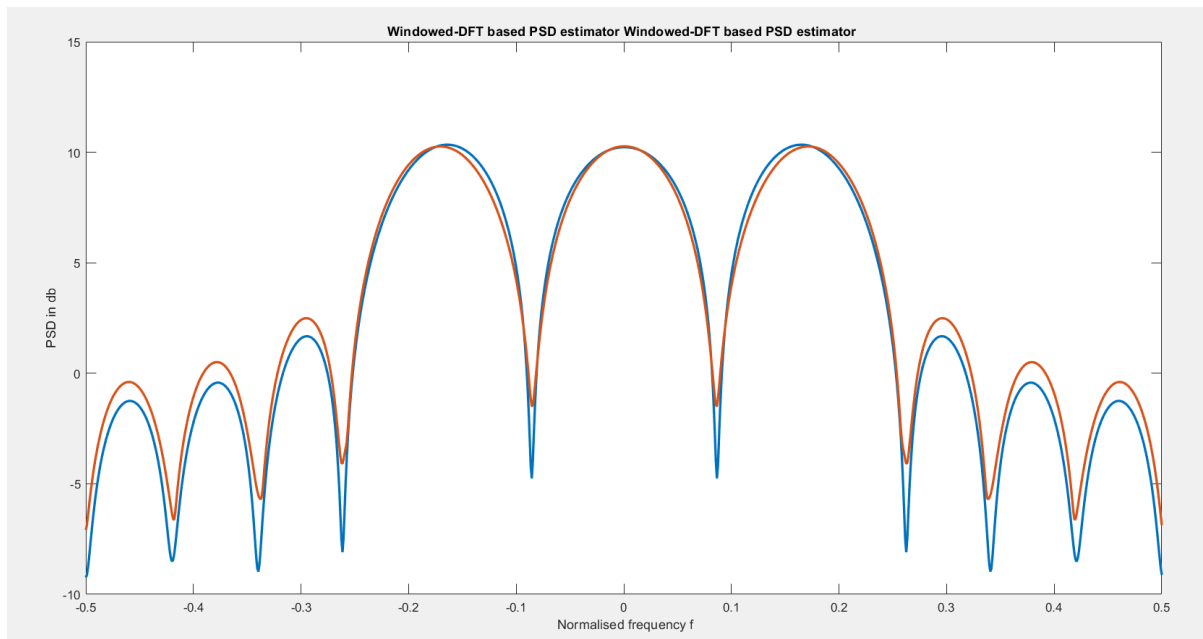


Figure 5-1 DFT based PSD estimation

We observe peak values at the desired frequency, but we also follow several side lobes, undesired.

5.2 Windowed-DFT based PSD estimator

Kaiser Window with $\beta=1.2$



The Kaiser window minimizes the sidelobes but always at the expense of broadening the main lobe. By windowing, we are getting a better response for matched filtering. The estimate is not ideal, and it is affected by the problems of limited resolution, smearing, leakage, and estimation noise. These problems are typically mitigated if N can be increased per the requirement. However, in many issues of the practice, this is not feasible. The locations of the peaks of the PSD provide an estimate of the frequency of the narrowband signals present in the incoming signal sequence. The DOA estimator should be like a needle, a toothpick Sharp, and pointed at the location of the actual frequencies. Instead, it is like a finger (unless the incoming frequencies are truly cyclical given N). Smearly instead of pointed (low resolution, fuses the signals close in frequency). Surrounded by many other smaller fingers (weak signal suppression due to energy leakage in the sidelobes)

Chapter -6

6 Algorithms

6.1 Minimum Variance Distortion-less Response (MVDR) Method

We would like to have a filter w similar to the matched filter and reject the signals present at all other frequencies as much as possible. Since the signal at the output of the filter is $y_n = w^H x_n$ we would like to maximize $E[|y_n|^2]$ The power of the output signal and thus reject all the unwanted interference. However, we want to maximize the output contribution from the desired frequency f . This also avoids trivial solutions as we have seen that in Beamforming, the general inclination is to believe that the direction from where the power is arriving will give us the most substantial beam. The degree of freedom available is generally one less than the number of sensors. With the perception stated above, all the degrees of freedom are used to bolster the beam strength in the look direction. The thought is that maximum power would be achieved when the look direction coincides with the true DOA. The problem arises when there is more than one signal. A particular way is to use some degrees of freedom to form a beam in the look direction. The remaining should be used to create nulls in other directions, taking care of other signals. If we minimize the output power and inhibit the beam in the look direction or maintain unity gain, we can prevent the trivial solution $w=0$. This can also complete the need to form nulls from where other signals are coming. Thus Capon method uses degrees of freedom for two tasks. One is to minimize the array processor output power. $\min w^H \langle |y_n|^2 \rangle_N$ subject to $w^H a(\theta) = 1$. This method is also called MVDR- Minimum variance distortion-less response. This name can be justified as the minimum variance is achieved by minimizing the average power. Simultaneously, maintaining unity gain in the look direction gives you a distortion-less signal.

6.2 Mathematical model

The array output signal $y(n)$ variance is minimized, and the signal from the look direction with no distortion is unity gain, and no phase shift is passed. The weighing vector

$w_c(\theta)$ would be

$$w_c(\theta) = (a^H(\theta)R_{xx}^{-1}a(\theta))^{-1}R_{xx}^{-1}a(\theta) \quad (24)$$

Capon's method will search over all thetas to find the direction for which the measured power received is maximum.

$$P_c(\theta) = w_c^H(\theta)R_{xx}w_c(\theta) = (a^H(\theta)R_{xx}^{-1}a(\theta))^{-1} \quad (25)$$

Though we are not finding the maximum likelihood estimator of θ , this algorithm still considers Capon's entire likelihood method. This is because $P_c(\theta)$ is the complete likelihood estimate of a signal's signal power arriving from angle θ in the presence of temporal white Gaussian noise having arbitrary spatial characteristics. The emphasis is on $P_c(\theta)$ calculated using the estimated auto-correlation matrix. This is nothing but the pointwise maximum likelihood estimate of the angular density of received power. We can see the performance improvement when compared to the conventional beamforming algorithm.

6.3 Simulation results

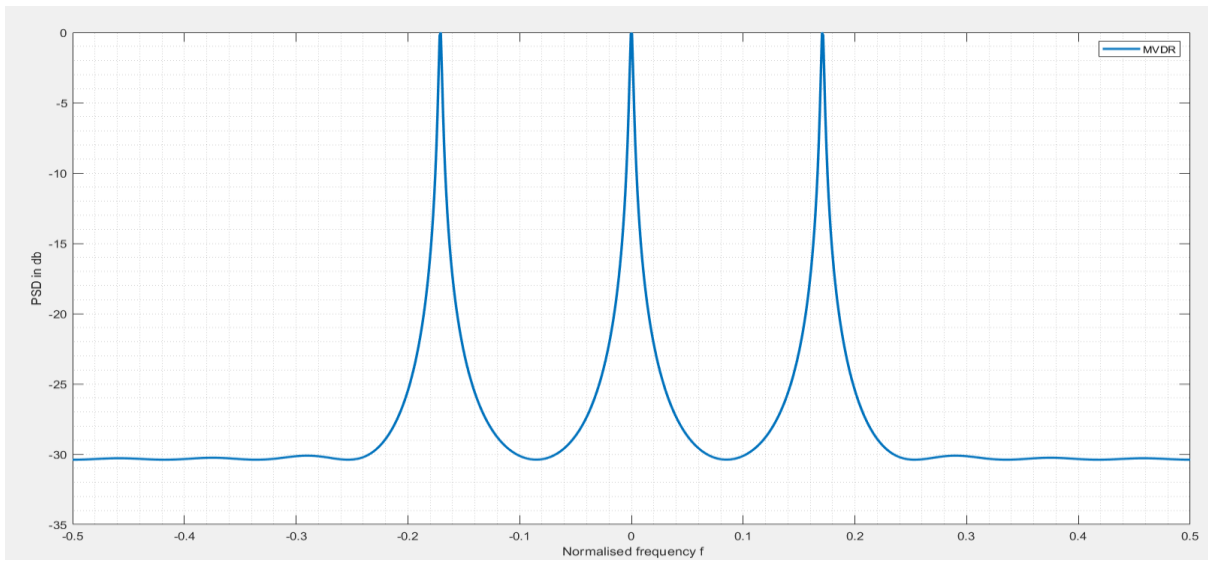


Figure 6-1 MVDR PSD for theta [-20, 0 ,20]

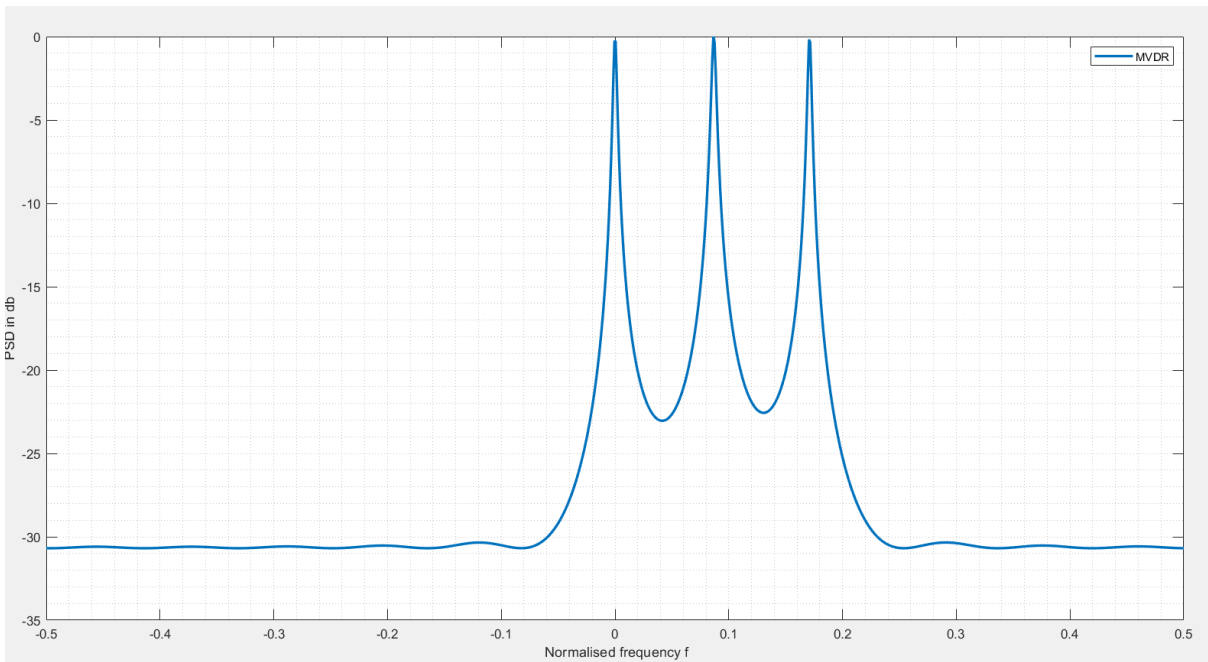


Figure 6-2 MVDR PSD for theta [0, 10 ,20]

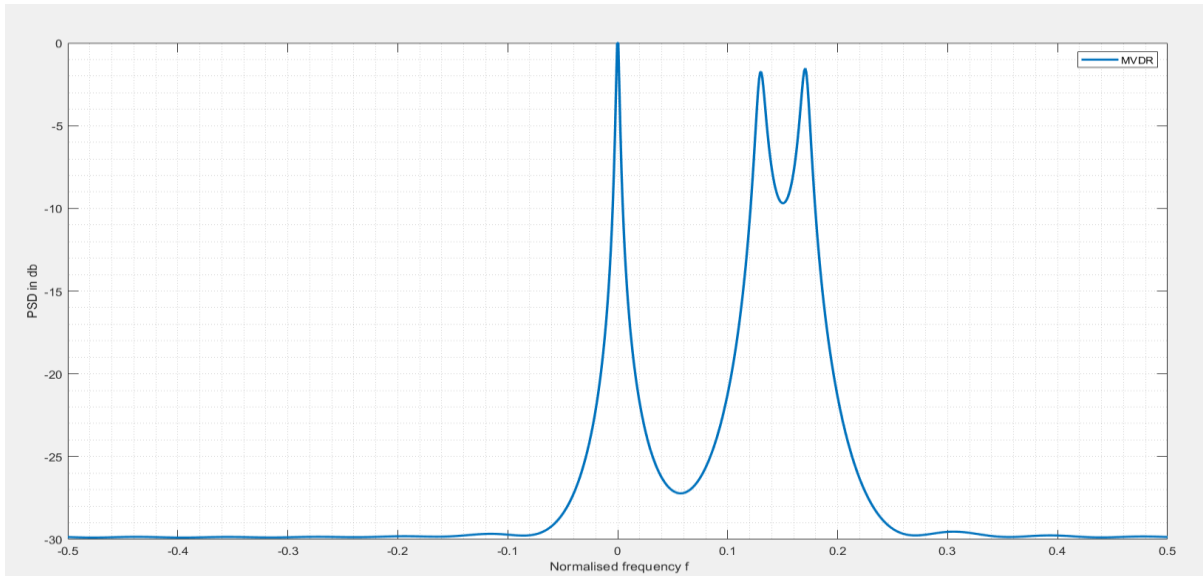


Figure 6-3MVDR PSD for theta [0, 15 ,20]

Figure 6.1 shows the simulation result for signals arriving from -20,0.20 degrees with carrier frequency $f=\sin(\theta)/2$, the total number of antennas 12, SNR around -20 0 20, the spacing of the elements in the array is kept as half the value of the wavelength. We get three sharp peaks at the desired frequency of arrival in this case.

Fig 6.2 shows the simulation result for signals arriving from 0,10, 20 degrees with carrier frequency is $f=\sin(\theta)/2$, the total number of antennas 12, SNR around -20,0,20, the spacing of the elements in the array is kept as half the value of the wavelength.

Capon's method also succumbs once we expect more accuracy and go below the range of 10 degrees spacing of signal sources.

Fig 6.3 shows the simulation result for signals arriving from 0,15, 20 degrees with carrier frequency is $f=\sin(\theta)/2$, the total number of antennas 12, SNR around -20,0,20, the spacing of the elements in the array is kept as half the value of the wavelength. Here MVDR performance degraded.

Suppose two closely spaced sources have signals which are perfectly co-related. In that case, this method will not spatially null either signal as it can just destructively

add them to reduce the final power output. The peaks would just merge to give a single height somewhere between the actual direction of the arrival angle.

6.4 The MUSIC algorithm

The earlier methods failed when the sources were closely located or the incoming signals were highly correlated. In those algorithms, a constant trade-off goes on between forming a solid beam in the look direction, attenuating other movements, and maintaining a low side lobe to attenuate noise. This happens because the received data autocorrelation matrix structure is overlooked. The matrix constitutes a full-rank autocorrelation matrix of the noise and unwanted signals and a low-rank autocorrelation matrix of desired signal components. The earlier algorithm also fails to detect the difference between when a signal is rejected due to spatial nulls and when it is rejected due to the destructive combination of correlated signals. These conditions are generally encountered in multipath propagation and signal jamming situations. These super-resolution algorithms jointly estimate the parameters for all signals in contrast to the previous algorithms[11]. This is done by taking advantage of the structure of the autocorrelation matrix. In addition to it, rather than directly working on the data, these algorithms might also use Beamforming and nulling in subspaces of the received data. The conclusions are obtained from the spatial filtering algorithm, but these concepts are more of a fit for subspace fitting.

The Multiple Signal Classification (MUSIC) proposal opened a new era for spatial spectrum estimation. The promotion of the algorithm's structure characterized rise and progress and became critical for the theoretical system of the spatial spectrum. The intention is to conduct characteristics decomposition for the covariance matrix of the processor output data. This results in a signal subspace that is orthogonal to the noise subspace. The direction of arrival is estimated using this orthogonal subspace.

Let us consider a model. R_{xx} is the autocorrelation matrix of the received data. We can get the desired signal components by subtracting R_{ii} , the autocorrelation matrix of the interference from R_{xx} . [11]

Given a weight vector w , the output power coming from the desired signal can be expressed as

$$P = w^H (R_{xx} - R_{ii}) w = w^H A(\Theta) R_{ss} A(\Theta)^H w \quad (26)$$

similarly, the sum of the average powers of the K outputs due to the desired signals would be

$$P_{\text{total}} = \sum_{k=1}^K P_k = \text{tr}[w^H (R_{xx} - R_{ii}) w] \quad (27)$$

$W = [w_1 \cdots w_K]$. Just as when we limit the narrowness of the transition band of an FIR filter by applying the passband and stopband simultaneously, the resolution here can be limited by simultaneous operation of Beamforming and null-steering. Let's take the example of nulling all signals simultaneously. As power P is of the desired signal space, it can be seen as if no noise signals are present. Let's say M is the number of sensors and L is the number of signals. So if fewer than M signals are present which are not completely correlated, W can be selected such that it would be able to null all the signals simultaneously. As the signals are not fully correlated, they can be rejected by only forming spatial nulls. We can get K weight vectors where $K=M-L$ as they would be linearly independent of each other. We want an $M \times K$ matrix E where each column w_k , for ' k ' = 1, \cdots , K nulls all the desired signals.

This is achieved by subjecting that the W columns are linearly independent while minimizing the total average power P_{total} . This condition can also be seen as $w^H w =$

I. The direction of arrival estimation can now be done by searching over θ for those array vectors $a(\theta)$ for which $\|w^H a(\theta)\|^2 = 0$.

We searched for the directions where a null is seen simultaneously in all $K=M-L$ vectors. Similarly, we can choose W -beam, for which we get the maximum total average output power P total. Thus MUSIC algorithm can be seen as having the following steps. The first step is to estimate the autocorrelation matrix R_{xx} using finite N .

The principle and implementation of the MUSIC algorithm MUSIC can estimate the DOA of multiple signals. These estimations are precise and are applicable for short data circumstances as well.

6.5 Implementation steps

While using this method, we need to take care of certain restrictions to precisely determine the results. The conditions for the MUSIC algorithm to function properly are

- 1) The number of signals says L should be less than the total number of sensors taken as M .
- 2) Within a given multiplicative constant, we need to know R_{ii} .
- 3) The autocorrelation matrix R_{ss} Which belongs to the signal should have a total rank, L .

A significant difference in MUSIC and the previous spatial filtering-based algorithm has seen the weight vectors here and then finds out the beams or nulls. In contrast, a new weight vector was computed for every direction in the earlier method.[12]

Basically, in MUSIC, all desired signals are jointly processed, and then processing is done to locate the DoA. Whereas the previous algorithms would estimate the DoA of one signal, and while doing so for the next signal, all these other signals are not

considered. In return, this gives us better performance than the MVDR method or the conventional beamforming method.

6.6 Simulation results

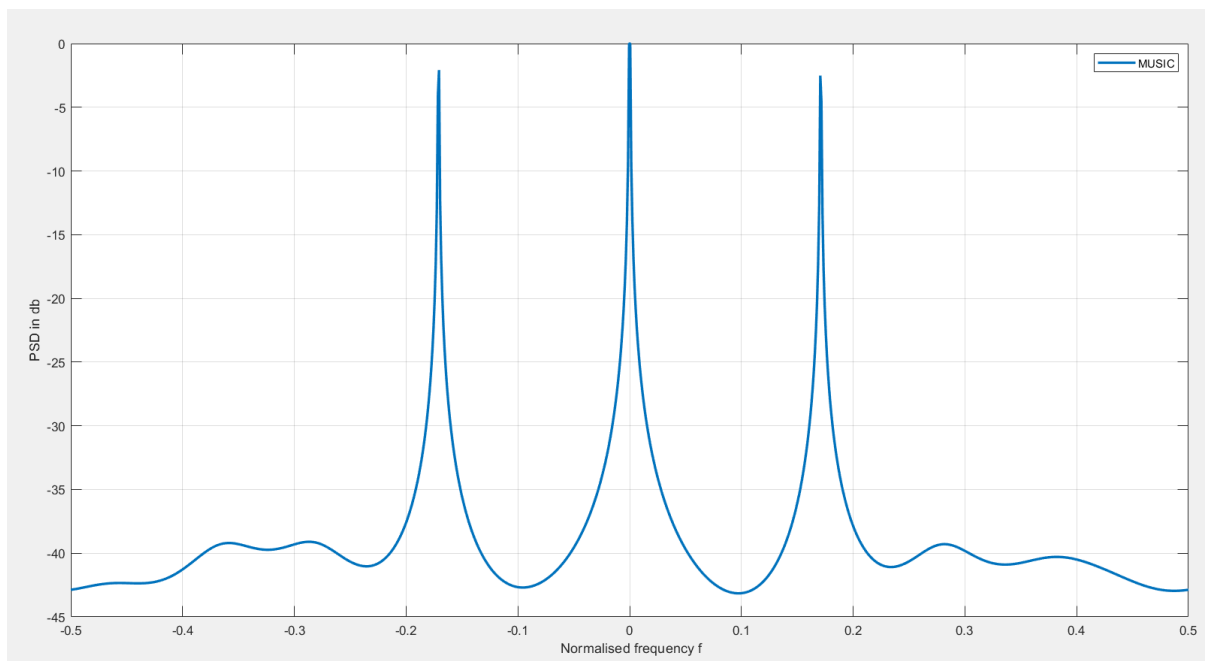


Figure 6-4 MUSIC PSD simulation for theta [-20.0.20]

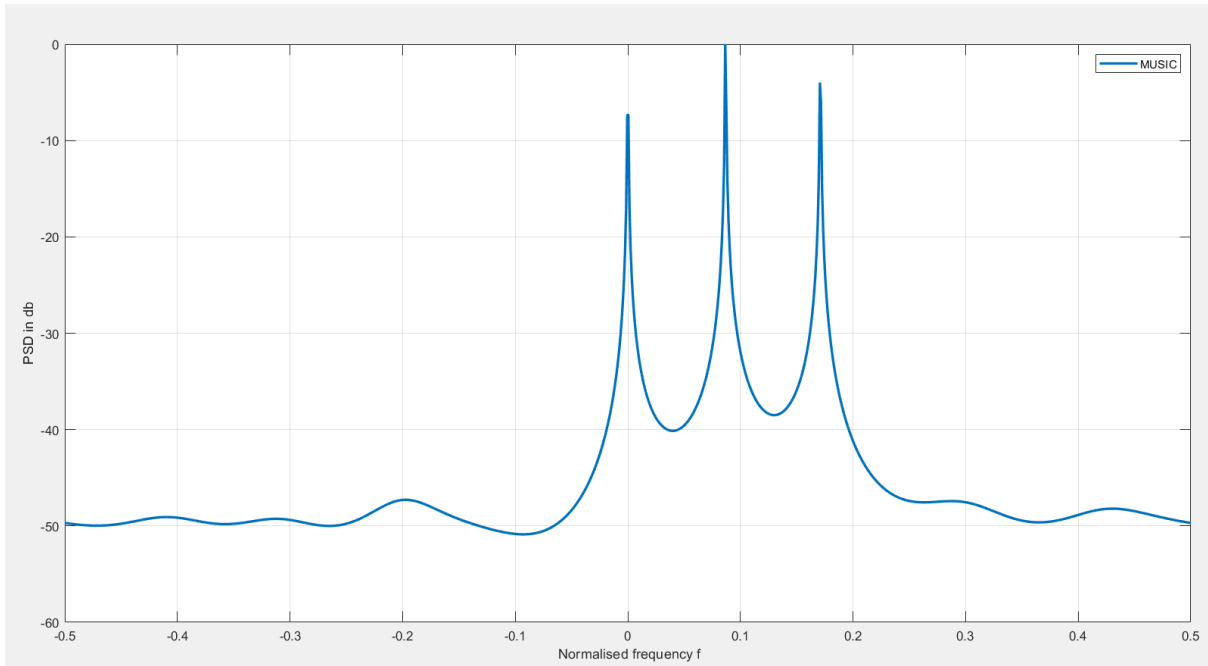


Figure 6-5 MUSIC PSD simulation for theta [0.10.20]

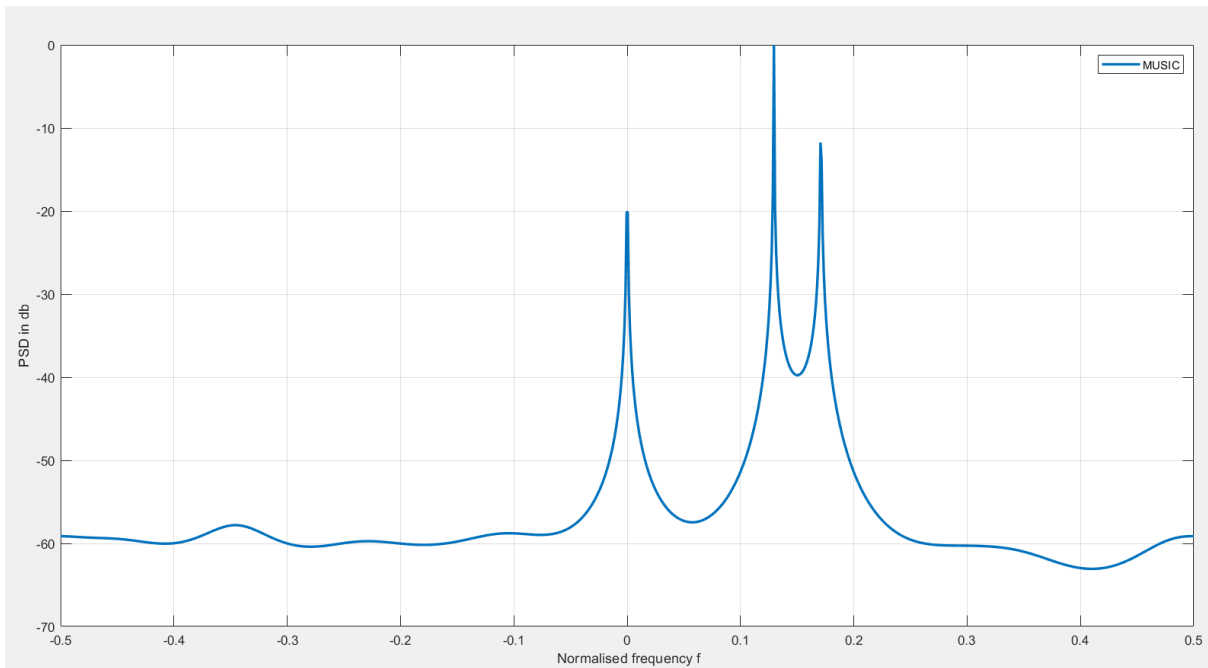


Figure 6-6 MUSIC PSD simulation for theta [0.15.20]

Figure 6.4 shows the simulation result for signals arriving from $-20, 0, 20$ degrees with carrier frequency $f = \sin(\theta)/2$, the total number of antennas 12, SNR around $-20, 0, 20$,

the spacing of the elements in the array has been kept as half the value of the wavelength. We get three sharp peaks at the desired frequency of arrival in this case.

Figure 6.5 shows the simulation result for signals arriving from 0,10.20 degrees with carrier frequency $f = \sin(\theta)/2$, the total number of antennas 12, SNR around -20 0 20, the spacing of the elements in the array is kept as half the value of the wavelength. We get three sharp peaks at the desired frequency of arrival in this case and thus demonstrate better results for closely spaced sources in a range of 10 degrees.

Figure 6.6 shows the simulation result for signals arriving from 0,15.20 degrees with carrier frequency $f = \sin(\theta)/2$, the total number of antennas 12, SNR around -20 0 20, and the spacing elements in the array is kept as half the value of the wavelength. We get three sharp peaks at the desired frequency of arrival in this case. The earlier drawback with very closely spaced sources not resolved in the simulation result shown in figure 6.3 has been removed using MUSIC methods as shown in figure 6.6. The range of the signal sources here is less than 10 degrees. MUSIC method also fails when you have fully co-related signals or multipath cases—several approaches like spatial smoothing overcome this.

6.7 Expectation-Maximization Algorithm

DOA Estimation as Sparse Signal Estimation Problem MMV Schematic. The main goal is to estimate $E[|z_m|^2]$ for $m=1,2,\dots,M$. Ideally $E[|z_m|^2] = 0$ only for those z_m which equals one of s_k Elements. These locations indicate which columns of A are present in W , thereby solving the DOA problem[5]

Initialize the \mathbf{R}_{zz} Is taken as a randomly generated diagonal matrix. Construct the MVDR filter corresponding to each DOA for all m. Using the estimate of \mathbf{R}_{zz} in the prior iteration to obtain an estimate $R_{xx,m}$ and using $R_{xx,m}$ construct the mth MVDR filter.

$$R_{xx,m} = \mathbf{w}_m^H(\theta) \mathbf{R}_{xx} \mathbf{w}_m(\theta) \quad (28)$$

Obtain the MVDR output for each P MMVs for the given theta. Take $y_{p,m}$ as an estimate of z_m At the frequency, f has given the Pth column of the MMV. Set the mth diagonal of \mathbf{R}_{zz} as

$$\frac{1}{P} \sum_{p=1}^P |y_{p,m}|^2 \cdot \quad (29)$$

6.8 Simulation result for Expectation Maximization

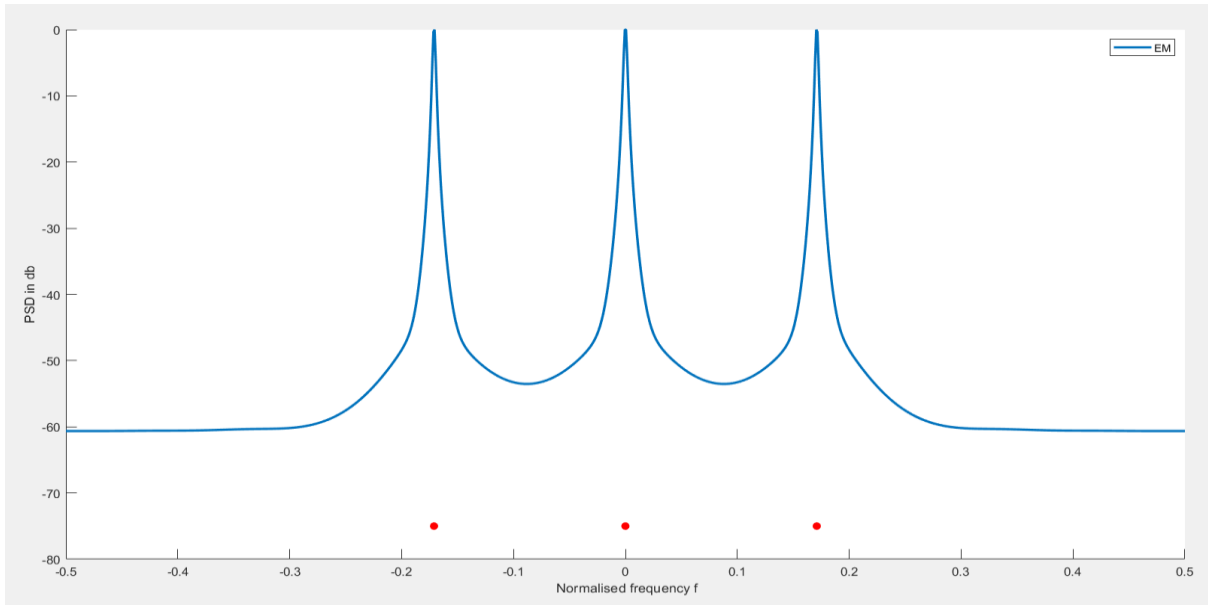


Figure 6-7 EM PSD simulation for theta [-20,0,20]

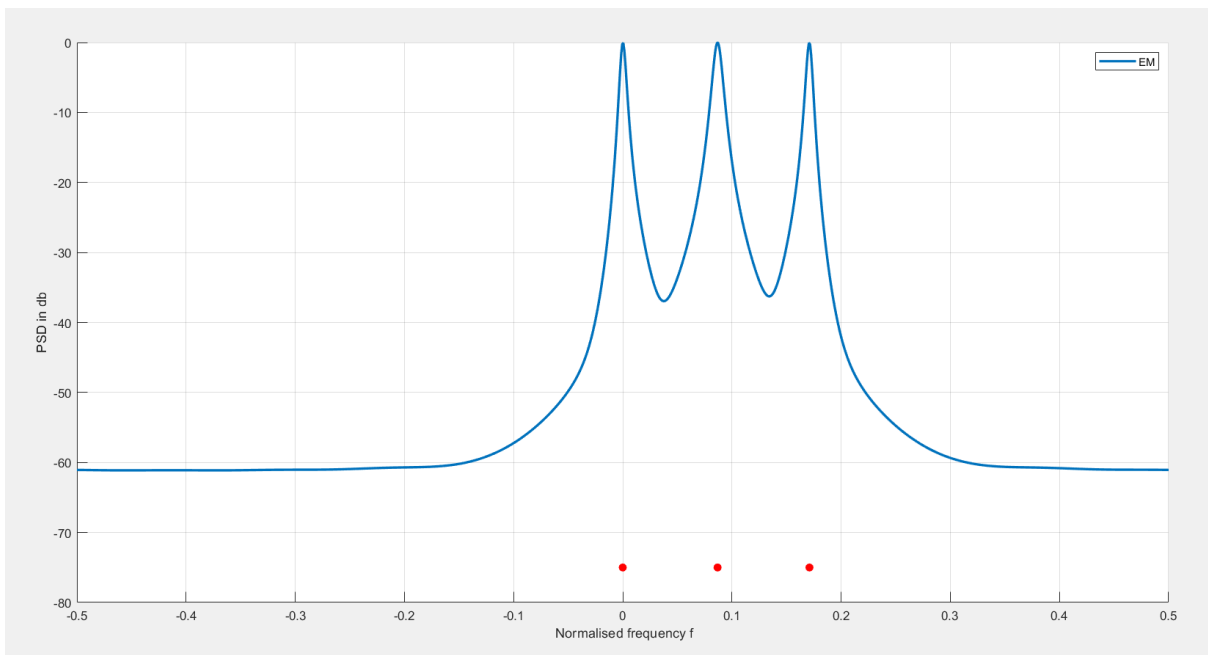


Figure 6-8 EM PSD simulation for theta [0,10,20]

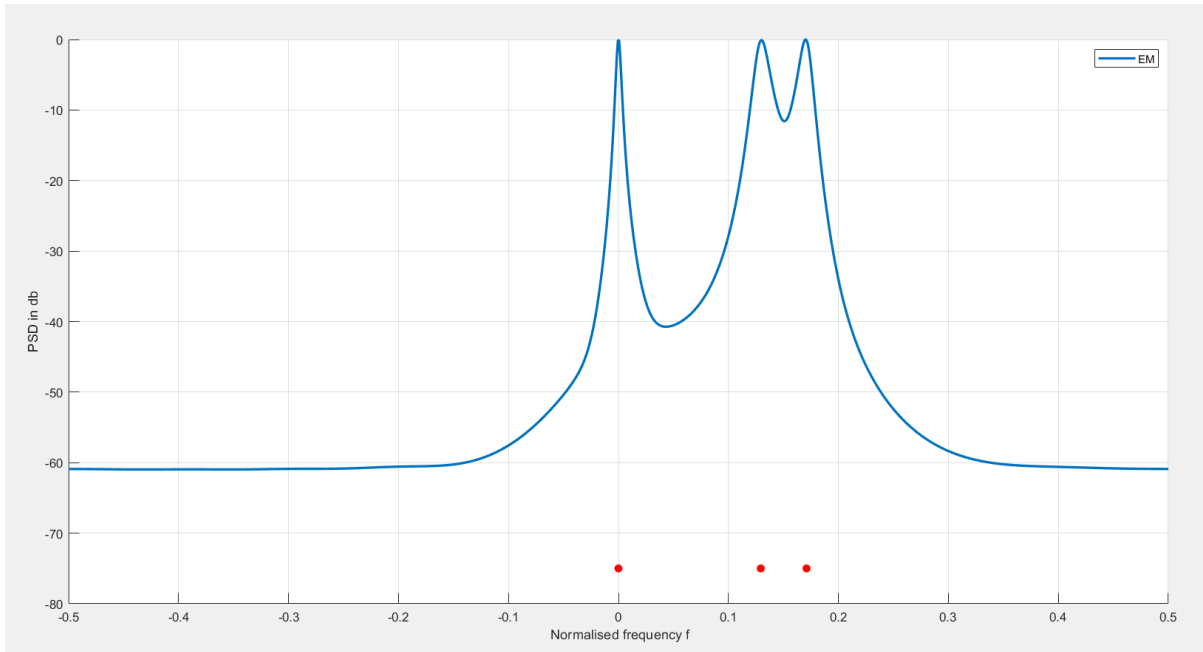


Figure 6-9 EM PSD simulation for theta [0,15,20]

Figure 6.7 shows the simulation result for signals arriving from $-20,0.20$ degrees with carrier frequency $f=\sin(\theta)/2$, the total number of antennas 12, SNR around -20 0 20 , and the spacing elements in the array is kept as half the value of the wavelength. We get three sharp peaks at the desired frequency of arrival in this case.

Figure 6.8 shows the simulation result for signals arriving from $0,10.20$ degrees with carrier frequency $f=\sin(\theta)/2$, the total number of antennas 12, SNR around -20 0 20 , and the spacing elements in the array is kept as half the value of the wavelength. We get three sharp peaks at the desired frequency of arrival in this case and demonstrate better results for closely spaced sources, which are in a range of 10 degrees.

Figure 6.9 shows the simulation result for signals arriving from $0,15.20$ degrees with carrier frequency $f=\sin(\theta)/2$, the total number of antennas 12, SNR around -20 0 20 , and the spacing elements in the array is kept as half the value of the wavelength. We get three sharp peaks at the desired frequency of arrival in this case. The earlier drawback with very closely spaced sources not resolved in the simulation result shown in figure 6.3 has been removed using the EM method, as shown in figure 6.9.

6.9 Comparative study of all algorithms

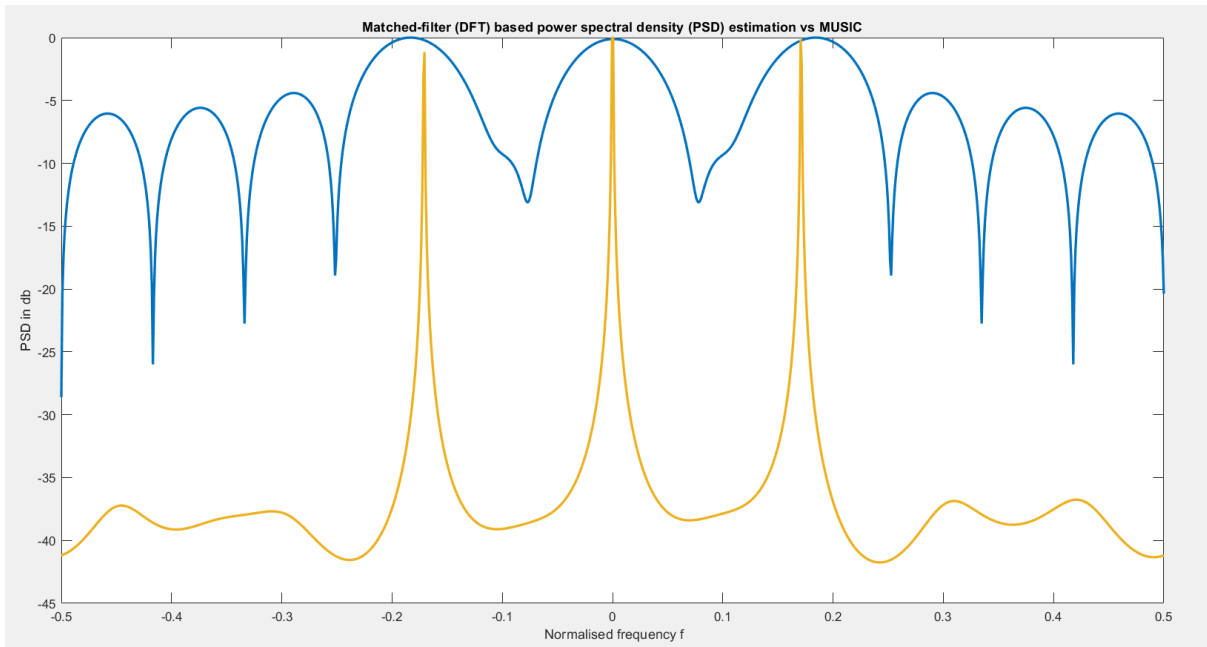


Figure 6-10 MF vs. MUSIC

When comparing MUSIC with matched filtering, we can see how better beams are formed by MUSIC. Beams are very narrow, so chances of interference will be less, and estimation is better

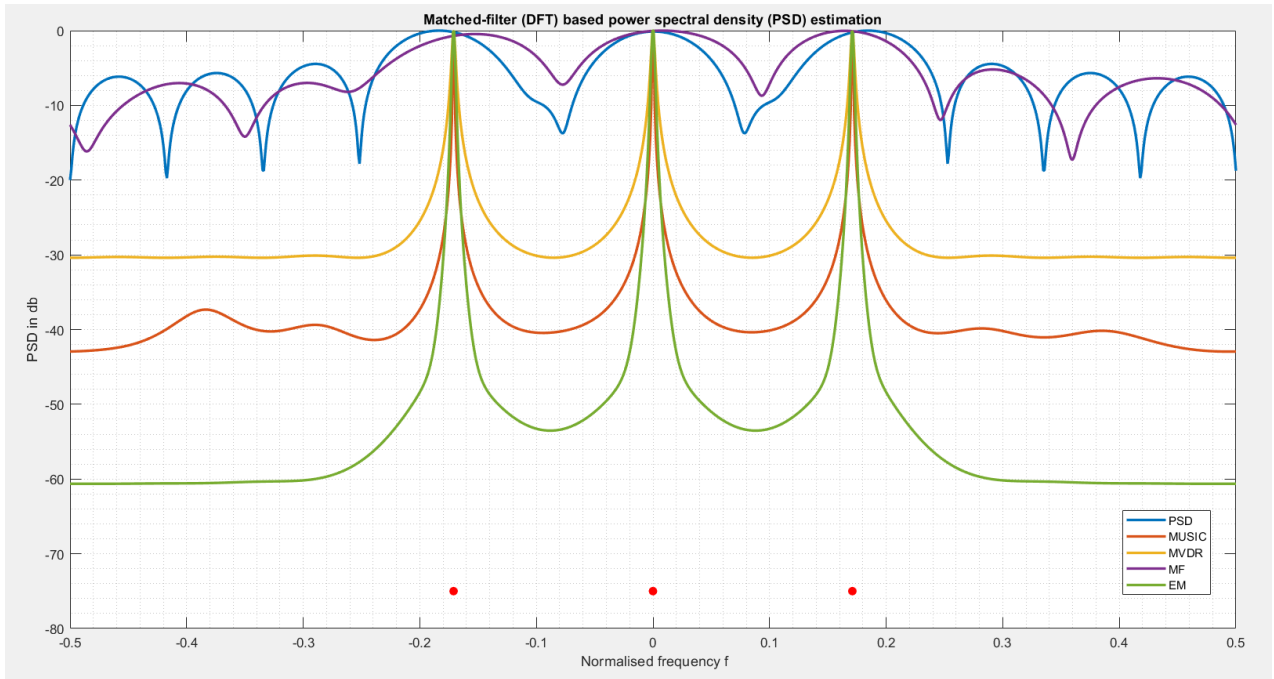


Figure 6-11 PSD for all algorithms

Estimation performance is better for EM, MUSIC, MVDR, while MF-based PSD performs worse.

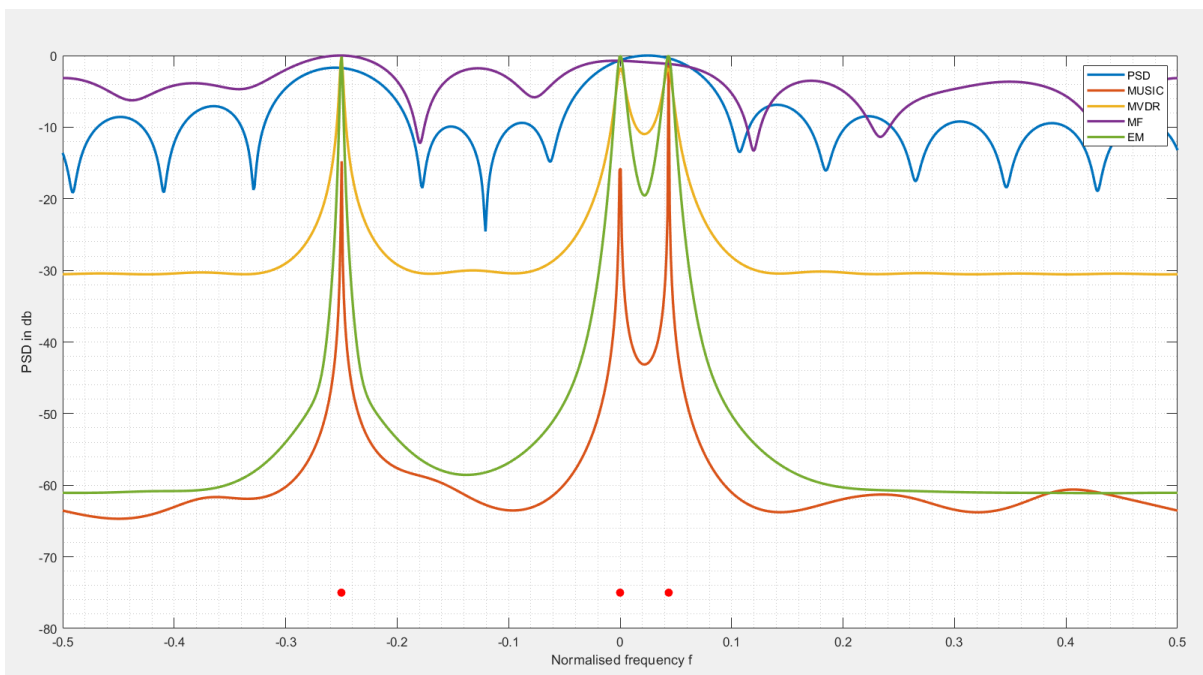


Figure 6-12 PSD for all algorithms when theta=-30,0,5

MUSIC, EM only can identify all three signals.

7 Uniform Planar Array

Formal investigation of smart antennas for wireless communication has primarily focused on uniform linear array (ULA) antennas, where multiple isotropic radiating elements are equally spaced in a line. A lot of DOA estimation algorithms have been proposed for ULA, such as matched filter (MF) DOA estimation, minimum-variance-distortionless response (MVDR) DOA estimation, multiple signal classification (MUSIC) DOA estimation. There are little attention and literature on DOA estimation with other smart antenna array topologies. Individual radiators are positioned along the rectangular grid for uniform planar array (UPA) antennas to form a planar array. Planar arrays provide additional variables which can be used to control and shape the pattern of the array. Hence they are more versatile and can provide more symmetrical patterns with the lower side [6]

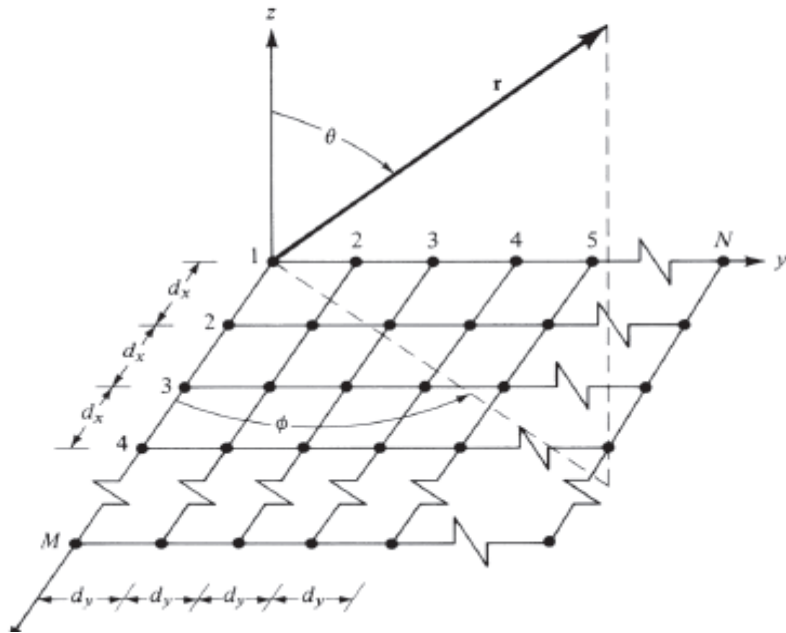


Figure 7-1 Rectangular array

7.1 Array Factor of Uniform Planar Array

M elements are placed on the x-axis and N elements at the y-axis with a uniform gap of d_x and d_y Equals 0.5

$$AF_x = \sum_{m=1}^M I_m e^{i(m-1)} (k d_x \sin \theta \cos \phi + \beta_{a_x}) \quad (30)$$

$$AF_y = \sum_{n=1}^N I_n e^{i(n-1)} (k d_y \sin \theta \cos \phi + \beta_{a_y}) \quad (31)$$

$$\begin{aligned}
 AF = \sum_{m=1}^M I_m e^{i(m-1) (k d_x \sin \theta \cos \phi} & \quad (32) \\
 + \beta_{a_x}) \sum_{n=1}^N I_n e^{i(n-1) (k d_y \sin \theta \cos \phi + \beta_{a_y})} &
 \end{aligned}$$

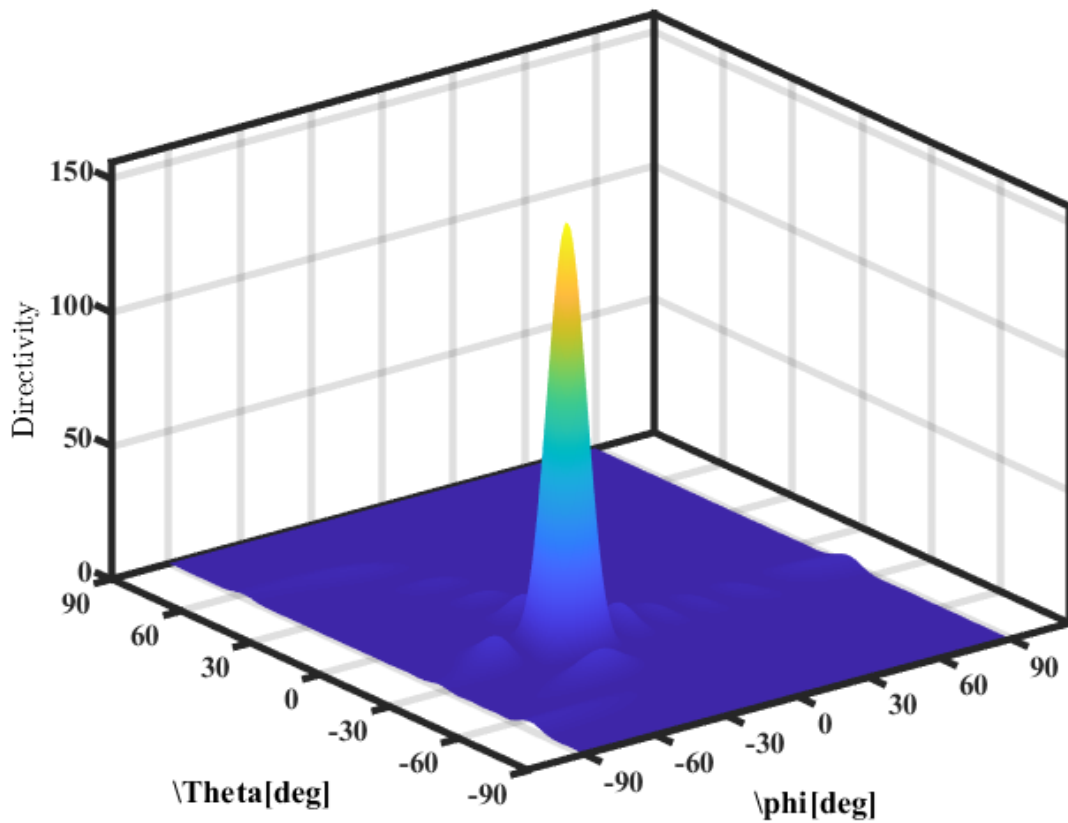


Figure 7-2 Array Factor of Uniform linear array for theta=30 and phi=45 for dx=dy=0.5

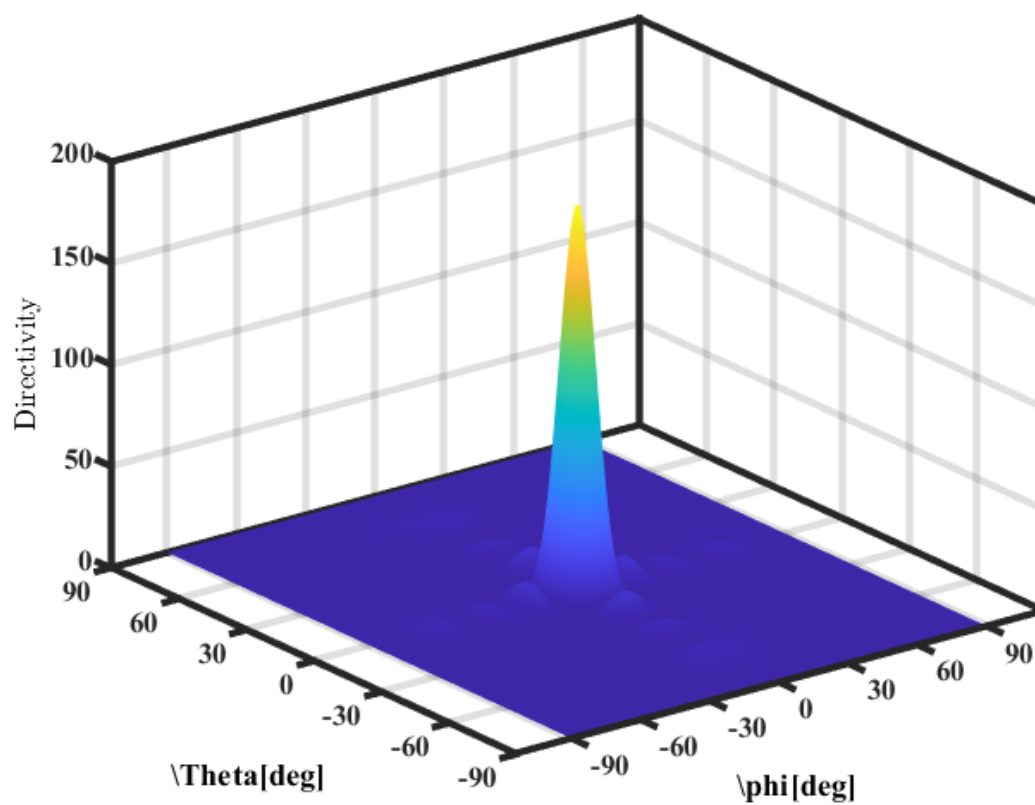


Figure 7-3 Array Factor of Uniform Planar array for $\theta=0$ and $\phi=0$ for $dx=dy=0.5$

The figure shows that the uniform array factor shows directivity when θ and ϕ are zero degrees.

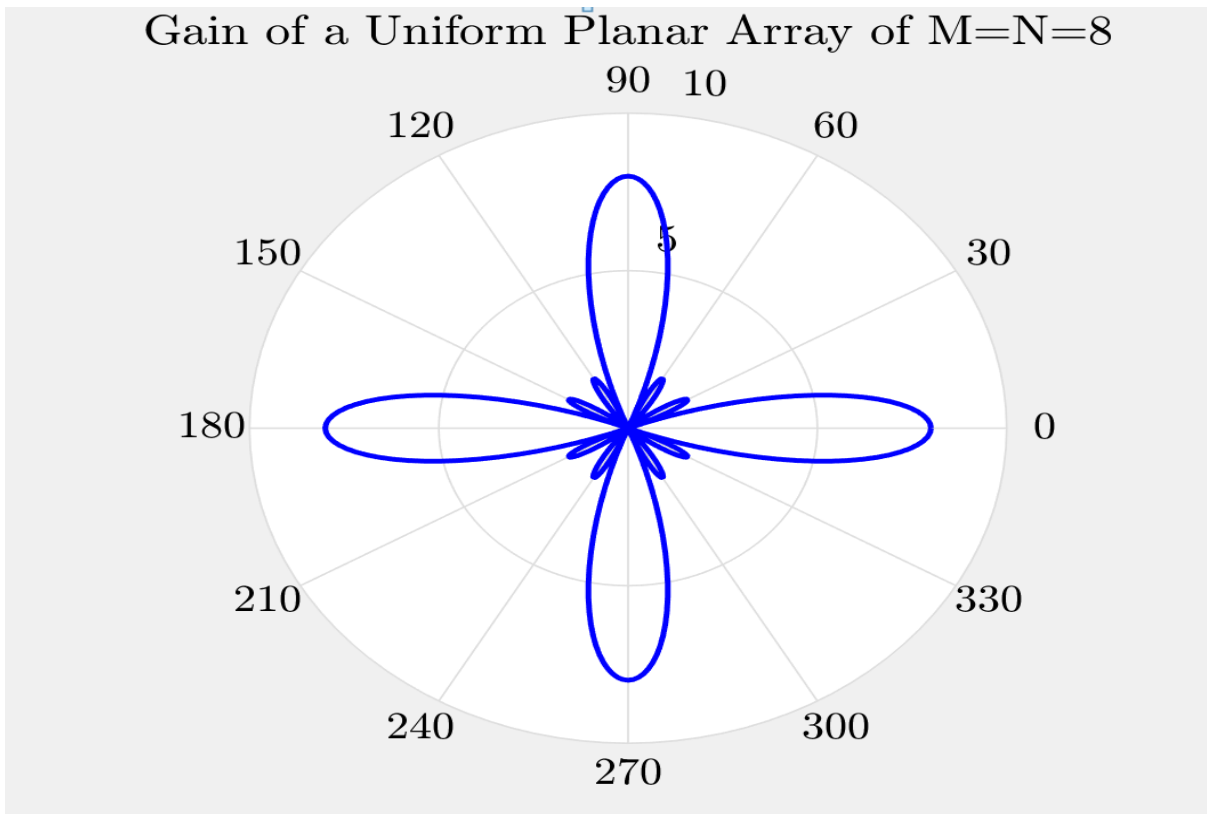


Figure 7-4 2-d Antenna radiation pattern for M=N=8 and $\theta = \phi = 0$

The figure shows the Polar Plot for Uniform planar array shows directivity when θ and ϕ are zero degrees.

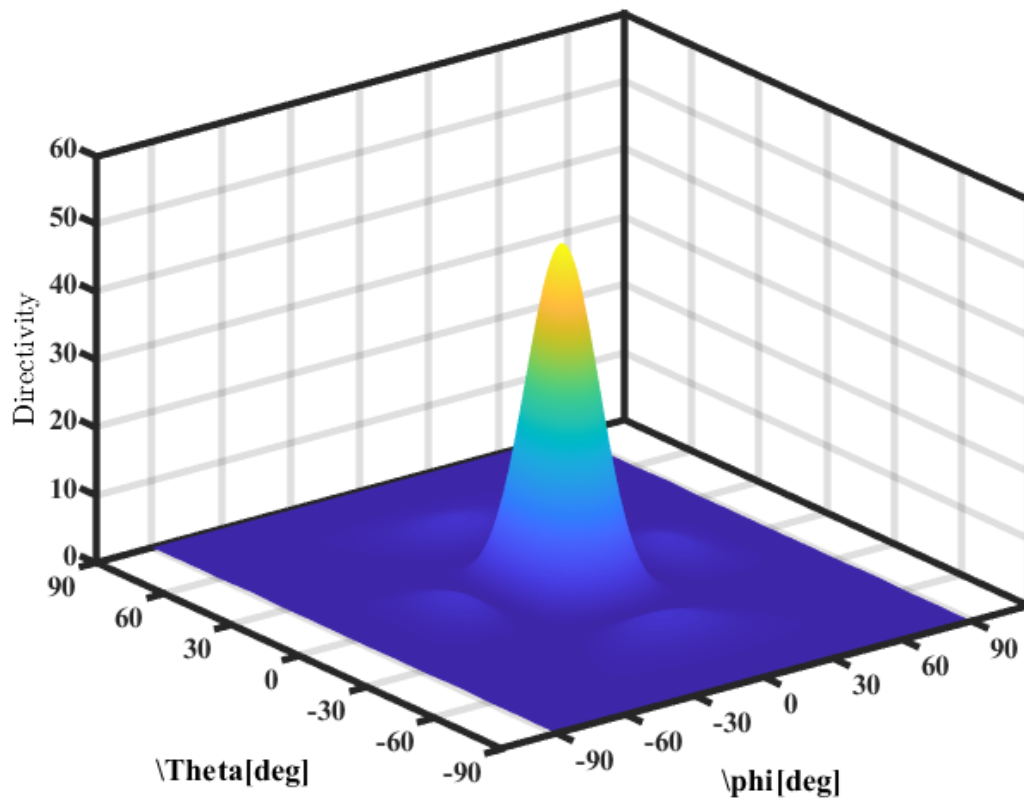


Figure 7-5 3-d Antenna radiation pattern of isotropic elements for $dx=dy=0.25$, θ and $\phi=0$

The figure shows directivity when d is less than 0.5 and thus leads to widening of spectral width.

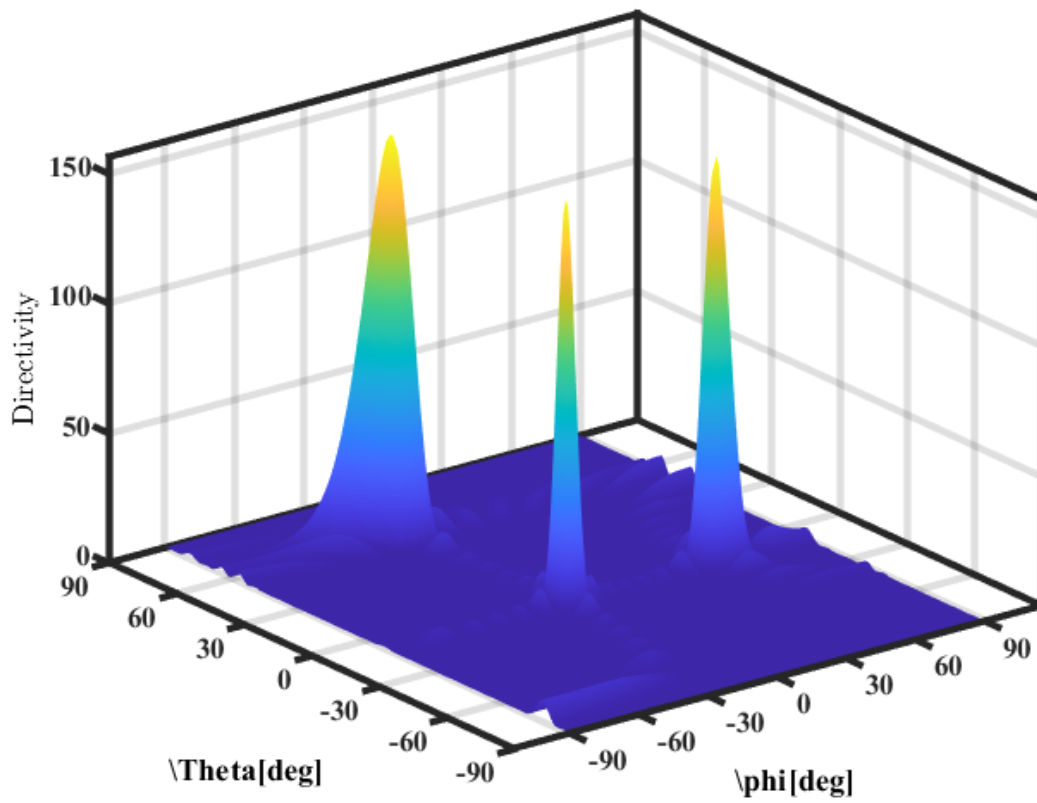


Figure 7-6 3-d Antenna radiation pattern of isotropic elements for $dx=dy=1$, $\theta=30$ and $\phi=45$

When d is greater than 0.5 thus replication of spectral beam will occur due to spectral aliasing.

8 UNIFORM CIRCULAR ARRAY

Uniform circular array (UCA) is an extraordinary planar array with many excellent properties over ULA. It can provide azimuthally coverage of 360 degrees and a certain degree of source elevation information.[7]

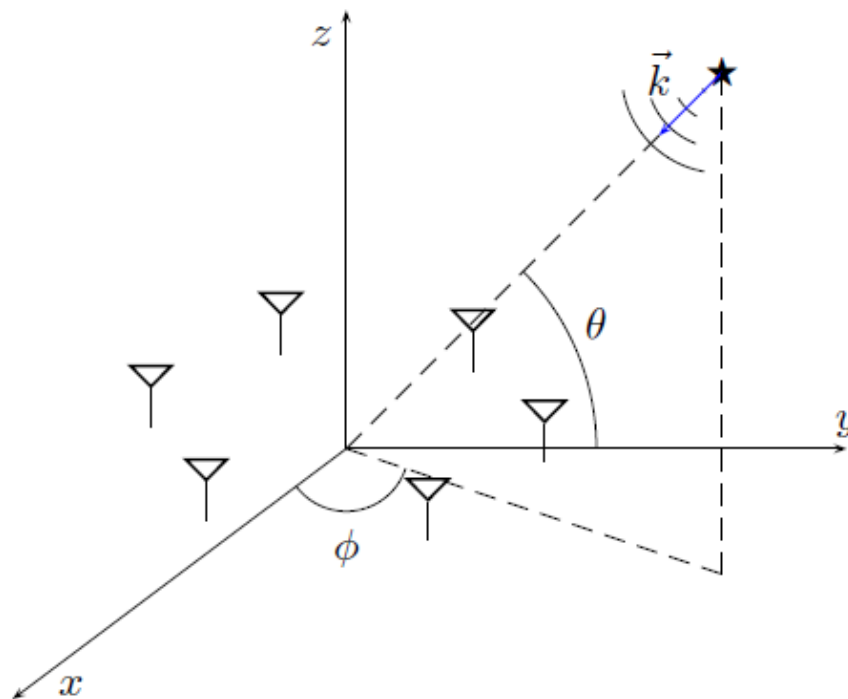


Figure 8-1 Uniform Circular Array

The array performs spatial sampling of a wavefront impinging from direction (θ, ϕ) and assumes a homogeneous propagation medium, a source in the far-field of the variety, and plane wavefront[8][9].

$$\tau_n = \frac{1}{c} [x_n \cos \theta \cos \phi + y_n \cos \theta \sin \phi + z_n \sin \theta]$$

$$a_n(\theta, \phi) = e^{i \frac{2\pi}{\lambda} [x_n \cos \theta \cos \phi + y_n \cos \theta \sin \phi + z_n \sin \theta]}$$

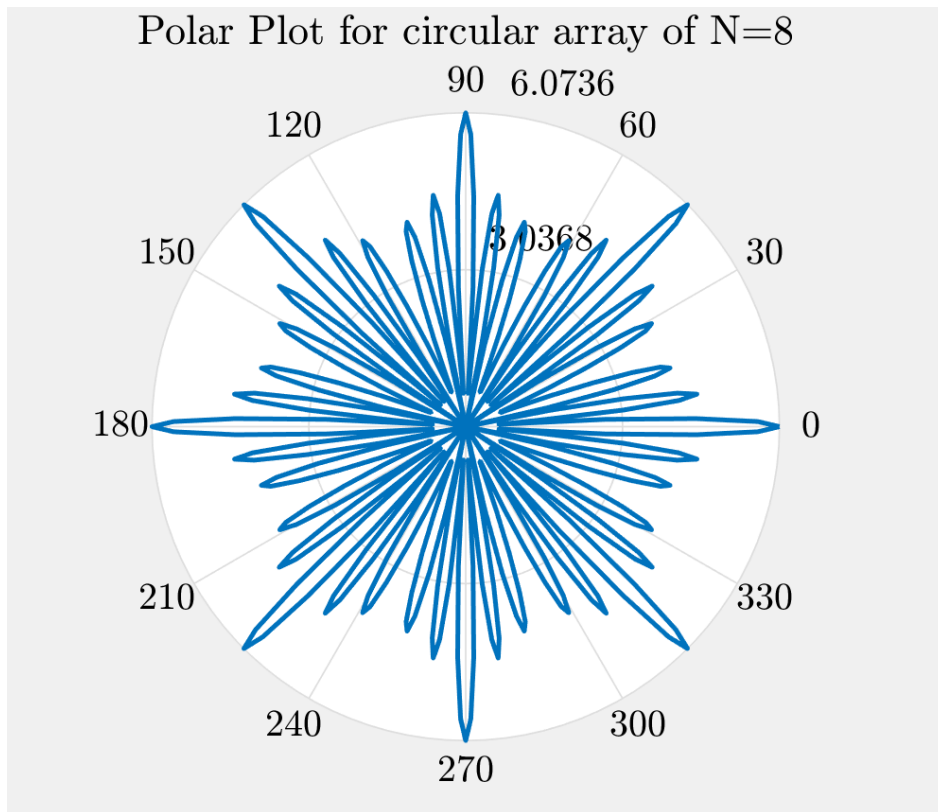


Figure 8-2 Polar Plot for N=8

8.1 MUSIC FOR UCA AND UPA

The N antenna elements are assumed to be omnidirectional, identical, and uniformly distributed over the circumference of a circle with the radius r in the X-Y plane. p equal powered sources arriving at the center of the circular array of radius $r=\lambda$ from the far-field with azimuth angle φ_k and elevation angle θ_k is shown in the figure below

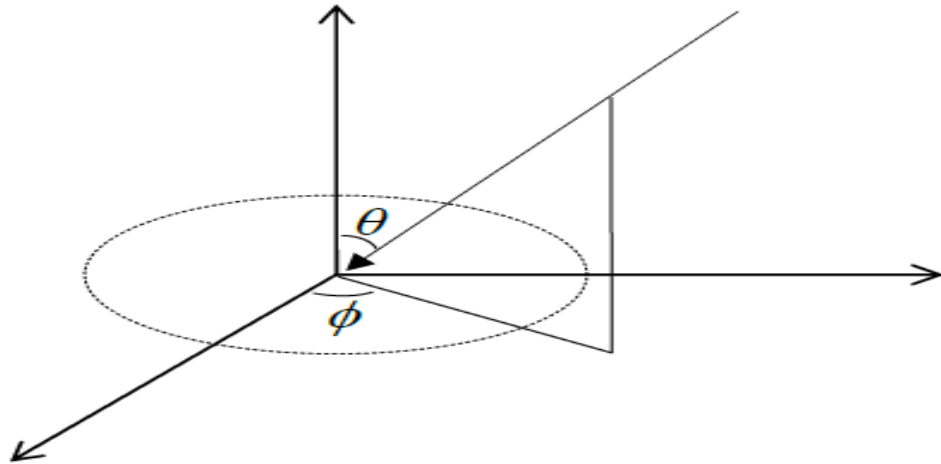


Figure 8-3 Uniform Circular array

We assume *The array observes k samples*, the antenna array output matrix is

$$X=AS+W$$

Where X is an NxK element space data matrix, A is an $N \times p$ element space array manifold, S is a $p \times K$ complex signal envelopes at the array center, W is the matrix of noise NxK complex envelopes. The signals and noise are assumed stationary zero mean, uncorrelated random processes. The element space array manifold matrix A is [8][10][11]

$$A= [a_1(\tau, \phi), a_2(\tau, \phi), a_3(\tau, \phi), a_4(\tau, \phi) \dots \dots \dots] \quad (33)$$

The column matrix is modeled as

$$a(\phi, \theta)= [e^{-j\theta \cos(\phi-\gamma_0)}, e^{-j\theta \cos(\phi-\gamma_1)}, e^{-j\theta \cos(\phi-\gamma_2)} \dots \dots \dots] \quad (34)$$

Where the elevation θ dependence through parameter τ and the vector $\theta = (\tau, \phi)$ is used to represent the source arrival directions [8][7][12]. Here $\zeta = k_o r \sin \theta$, $k_o = 2\pi/\gamma$ is wave number and r is the radius. $\gamma_n = 2\pi n/N$, ($n= 1,2,3,\dots,N$) is the sensor location.

A circle is periodic with period two π and can be represented in a Fourier series; each weight is called a phased mode in such series. To the Uniform circular array, the normalized beamforming weight vector with phase mode 'm' is

$$w_m^H = 1/N [1, e^{j2\pi m/N} \dots \dots \dots e^{j2\pi(N-1)/N}] \quad (35)$$

Let M denotes the highest order mode that can be excited by the aperture at a reasonable strength $M = k_0 r = 2\pi$ and $M1$ is the total number of excited modes, $M1 = 2M + 1$ when $N > 2M$, UCA array pattern for way 'm' is

$$f_c^m = w_m^H a_1(\tau, \phi) = j^{|M|} J_m(\tau) e^{jM\phi} \quad (36)$$

where $J_m(\tau)$ is the Bessel Function of the first kind of order m . The Beamforming matrix F_e^H can be defined as $F_e^H = C Q^H$ where

$$C = \text{diag}\{j^{-M} \dots \dots \dots j^{-1}, j^{-0}, j^{-1} \dots \dots \dots j^{-M}\} \quad (37)$$

$$Q = \sqrt{N} [W_{-M} \dots \dots \dots W_0 \dots \dots \dots W_M] \quad (38)$$

The beamspace manifold synthesized by

$$a_e^H = F_e^H a(\theta) = \sqrt{N} j_\tau v(\phi) \quad (39)$$

The azimuthal variation of a_e^θ is through the vector

$$v(\phi) = [e^{-jM\phi}, \dots \dots \dots e^{-j\phi}, e^{-j0}, e^{j\phi}, \dots \dots \dots e^{jM\phi}] \quad (40)$$

$$V = 1/\sqrt{M} [v_{\alpha_{-M}}, \dots \dots \dots v_{\alpha_0}, \dots \dots \dots v_{\alpha_M}] \quad (41)$$

Composed of Bessel functions, and it implicitly depends on elevation angle. The UCA Music algorithm employs the Beamformer F_r^H to make the transformation from element space to beam space and make its array manifold real, the Beamformer F_r^H defined as

$$F_r^H = V^H C Q^H \quad (42)$$

$$V = 1/\sqrt{M} [v_{\alpha_{-M}}, \dots, v_{\alpha_0}, \dots, v_{\alpha_M}] \quad (43)$$

$\alpha = 2 \frac{\pi i}{M1}$ where $i \in [-M, M]$ are the azimuthal rotation angles. Multiplying element space array manifold by Beamformer, we obtain real beamspace manifold $a(\tau, \phi)$ by beamspace F_r^H we obtain real beamspace manifold $b(\tau, \phi)$ is

$$b(\tau, \phi) = F_r^H a(\tau, \phi) = \sqrt{N} V^H J_\tau V(\phi) \quad (44)$$

The Beamformer F_r^H is applied over the element space data matrix \mathbf{X} , and then the resulting Beamspace data matrix is

$$Y = F_r^H X = F_r^H A S + F_r^H W \quad (45)$$

$$Y = B S + F_r^H W \quad (46)$$

Where B is the real-valued beamspace direction of arrival matrix containing $b(\tau, \phi)$ As its columns. The array output covariance matrix in the beamspace is

$$R_{YY} = E[Y^H Y] = B P B^H + \sigma^2 I \quad (47)$$

Where \mathbf{P} is the signal covariance matrix. Let $\mathbf{R} = \text{Re}\{R_{YY}\}$ denotes the fundamental part of the beamspace covariance matrix [10]. The real-valued eigenvalue decomposition of the matrix \mathbf{R} yield the beamspace signal and noise subspaces. Let \mathbf{E}_S and \mathbf{E}_N be orthonormal matrices that span the beam and noise subspaces, respectively [13]

$$E_S = [e_1, e_2, \dots, e_p], \quad E_N = [e_{p+1}, \dots, e_N] \quad (48)$$

The UCA MUSIC spectrum $P(\tau, \phi)$ is

$$\mathbf{P}(\boldsymbol{\tau}, \phi) = \frac{\mathbf{1}}{\mathbf{b}^T(\boldsymbol{\tau}, \phi) \mathbf{E}_N \mathbf{E}_N^H \mathbf{b}(\boldsymbol{\tau}, \phi)} \quad (49)$$

The spectrum has peaks corresponding to signal arrival directions.

8.2 SIMULATIONS

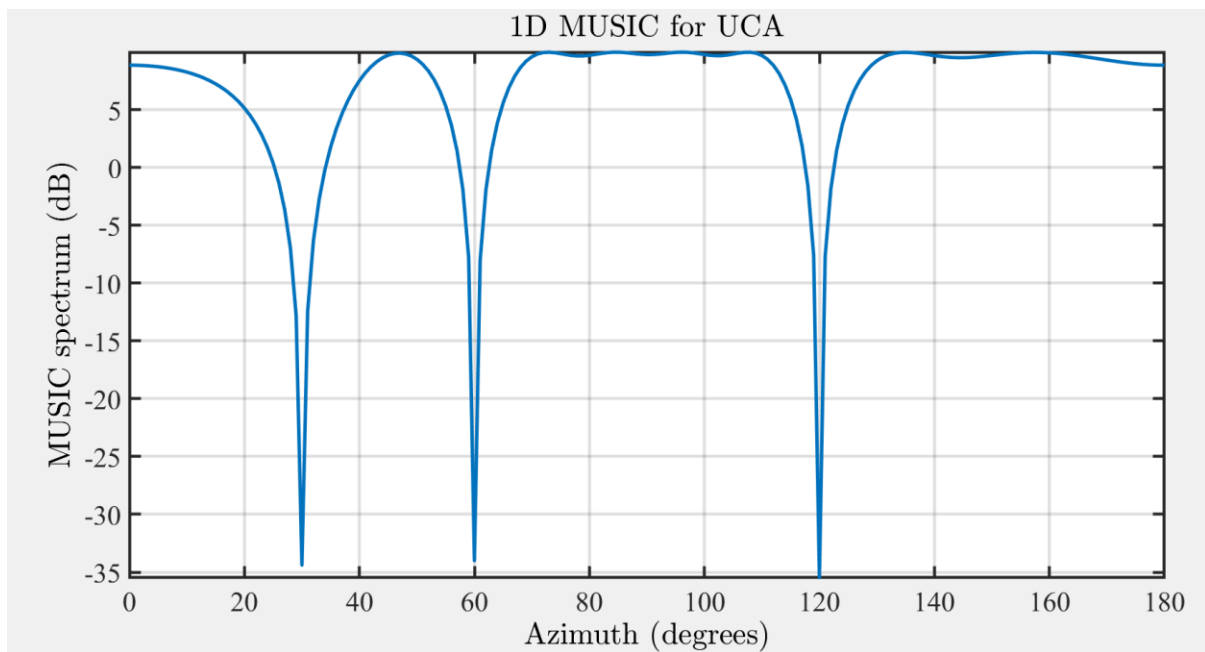


Figure 8-4:1-Dimensional MUSIC for UCA for DOA estimation of 30.60,120 degree

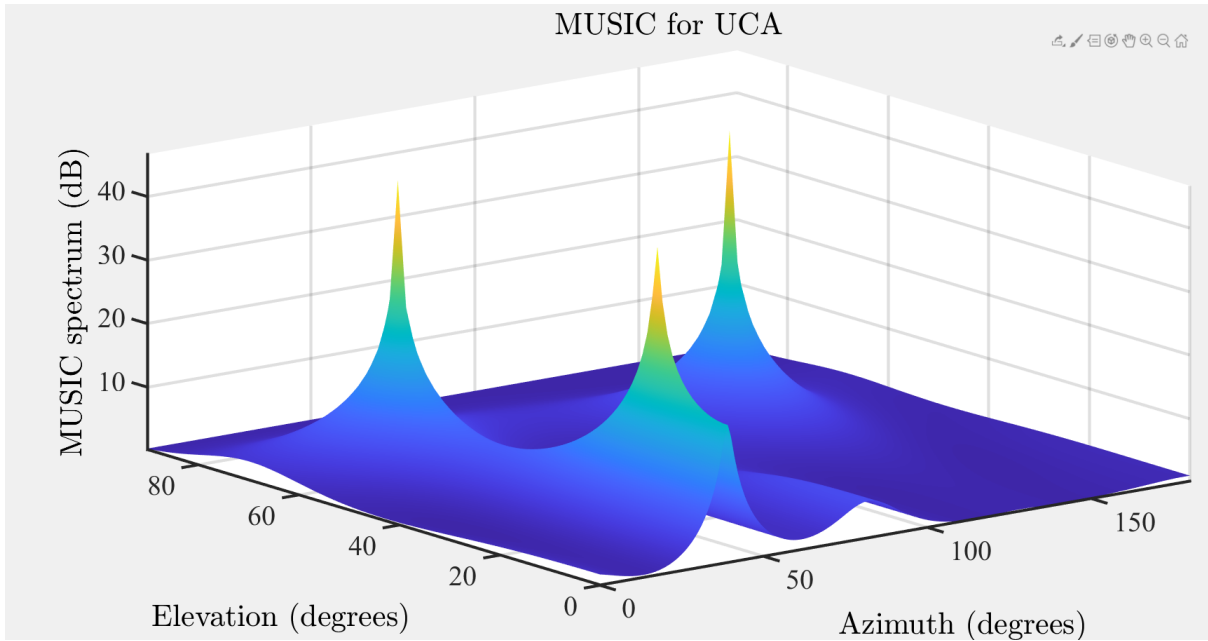


Figure 8-5 2-Dimensional MUSIC for UCA

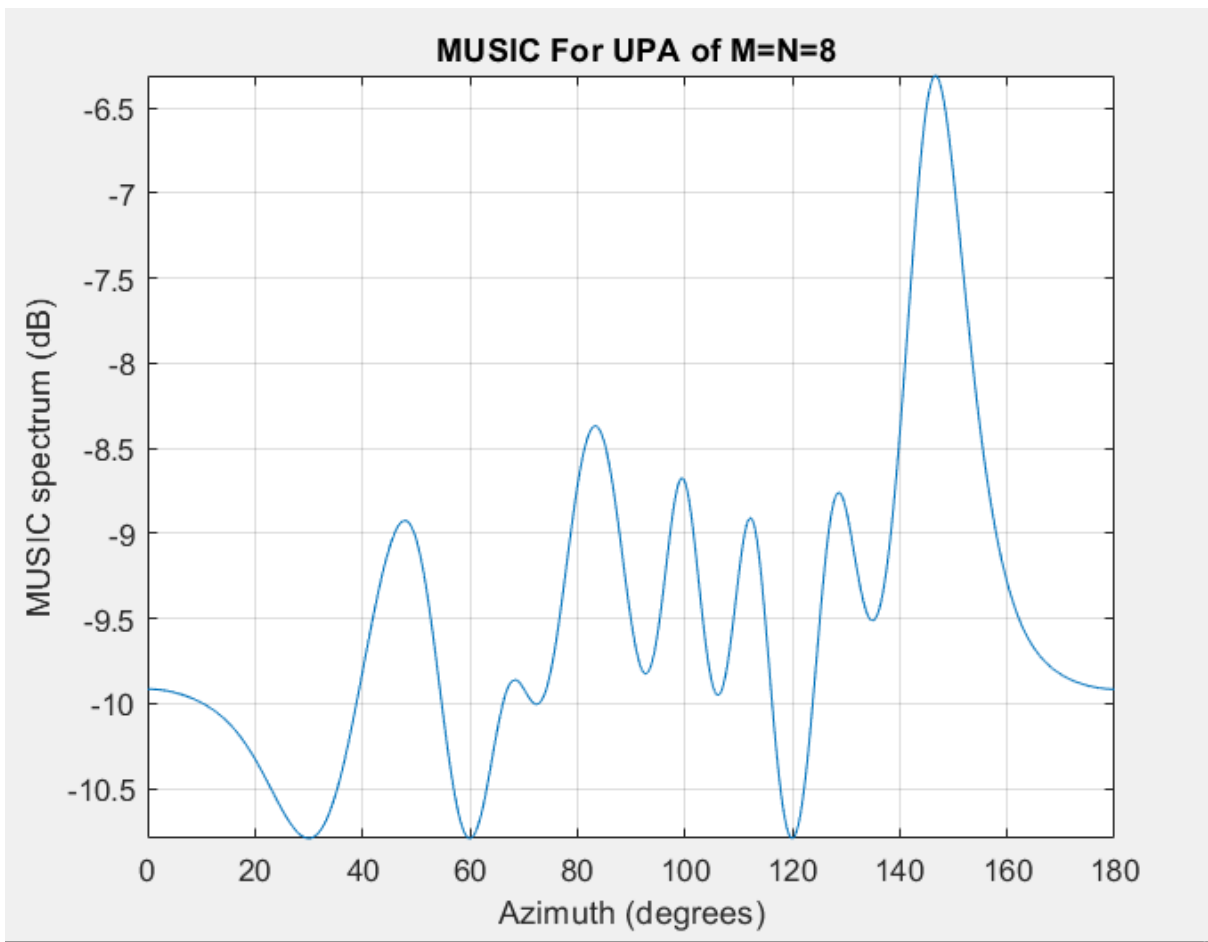


Figure 8-6:1-Dimensional DOA estimation for UPA for MUSIC algorithm for 30,60,120

9 Study Of Interference Cancellations Techniques

We have earlier considered the following model $N \times 1$ vector of the received signal samples with K simultaneous sources [14][15][16]:

$$\mathbf{X} = \sum_{k=0}^{K-1} w_N^{f_k} x_n^k + \mathbf{u} = \mathbf{W}\mathbf{s} + \mathbf{u} \quad (50)$$

The receiver is operating in real-time. A particular signal vector \mathbf{x} is observed at the input to the receiver. This signal is a composite of K source signals collected in a vector \mathbf{s} . One view: each source signal interferes with the others — since all K source signals are mixed up in the composite received signal. These source signals \mathbf{s} which carry the information, and our eventual interest is in demodulating these information-carrying symbols, i.e., We would like to estimate the symbol vector \mathbf{s} given the observed received vector \mathbf{x} . Another view: different source symbols together define a “super” (modulated) symbol (assumes that the different transmitters are synchronized). This is called the beamforming problem. In a generalized setting, also known as the source separation problem, this can be considered the demodulation problem in a further generalization. A typical assumption: FoA/DoA has been estimated. i.e., the elements of the matrix \mathbf{W} are known. In practice, this knowledge has some estimation errors.

The $N \times N$ correlation matrix of the incoming signal is given as

$$\mathbf{R}_{xx} = E[\mathbf{x}\mathbf{x}^H] = \mathbf{W}\mathbf{R}_{ss}\mathbf{W}^H + \sigma^2\mathbf{I}_N \quad (51)$$

The $K \times K$ spatial arrays are defined as $\mathbf{R} = \mathbf{W}^H\mathbf{W}$ assuming \mathbf{W} has a linearly independent column, and R is total rank, and it is inevitable

Let us perform the following operation on the received vector \mathbf{x} from the antenna array

$$\mathbf{Y} = \mathbf{W}^H\mathbf{x} = \mathbf{W}^H(\mathbf{W}\mathbf{s} + \mathbf{u}) = \mathbf{R}\mathbf{s} + \mathbf{v} \quad (52)$$

Where $W^H u = v$ is the transformed noise vector.

The $K \times 1$ vector y has a reduced dimensionality than the incoming signal vector since $K < N$. However, it is still capturing all the information present in the received signal vector x

Because x can be recovered from y since the correlation matrix is invertible and reduced dimensionality vector y is called sufficient statistics.

9.1 Least Square

The least-squares beamforming solution or decorrelator is

$$\mathbf{S} = \mathbf{R}^{-1} \mathbf{y} = \mathbf{s} + \mathbf{R}^{-1} \mathbf{v} \quad (53)$$

The interference among K signals is ideally removed. The estimated vector S becomes identical to the ideal s desired to be estimated without the noise.

9.2 MMSE solution

$$\mathbf{S} = (\mathbf{R} + \text{diag}\{\mathbf{1}/\gamma_s\})^{-1} \mathbf{y} \quad (54)$$

$\text{Diag}\{x\}$ denotes the diagonal matrix obtained by putting the elements of vector x along the diagonal [17]. Assume that the vector of SNRs of K users i.e

$\{\gamma_{sk} = E[|s_k|^2]/\sigma^2\}$ is known and that the noise is spatially uncorrelated.

The Correlation Matrix R is analogous to $R = H^H H$ and $y = R w$; therefore, MMSE

$$\mathbf{W} = \mathbf{R}^{-1} \mathbf{y} = (\mathbf{R} + \delta \mathbf{I}_K)^{-1} \mathbf{y} \quad (55)$$

The SUMF[18](Single User Matched Filter)

$$\mathbf{Y}=\mathbf{H}^H\mathbf{r} \quad (56)$$

Is the vector of decision variables used by the SUMF, and we have also called this sufficient statistics.

Least Square

$$\mathbf{S}=(\mathbf{H}^H\mathbf{H})^{-1}\mathbf{H}^H\mathbf{r} = \mathbf{R}^{-1}\mathbf{y} \quad (57)$$

Where R is the correlation matrix of H and y is the output vector.

MMSE

$$\mathbf{S}=(\mathbf{H}^H\mathbf{H} + \mathit{diag}\{1/\gamma_k\})^{-1}\mathbf{y}=(\mathbf{H}^H\mathbf{H} + \mathit{diag}\{1/\gamma_k\})^{-1}\mathbf{H}^H\mathbf{r} \quad (58)$$

9.3 Block Diagram of Beamformer

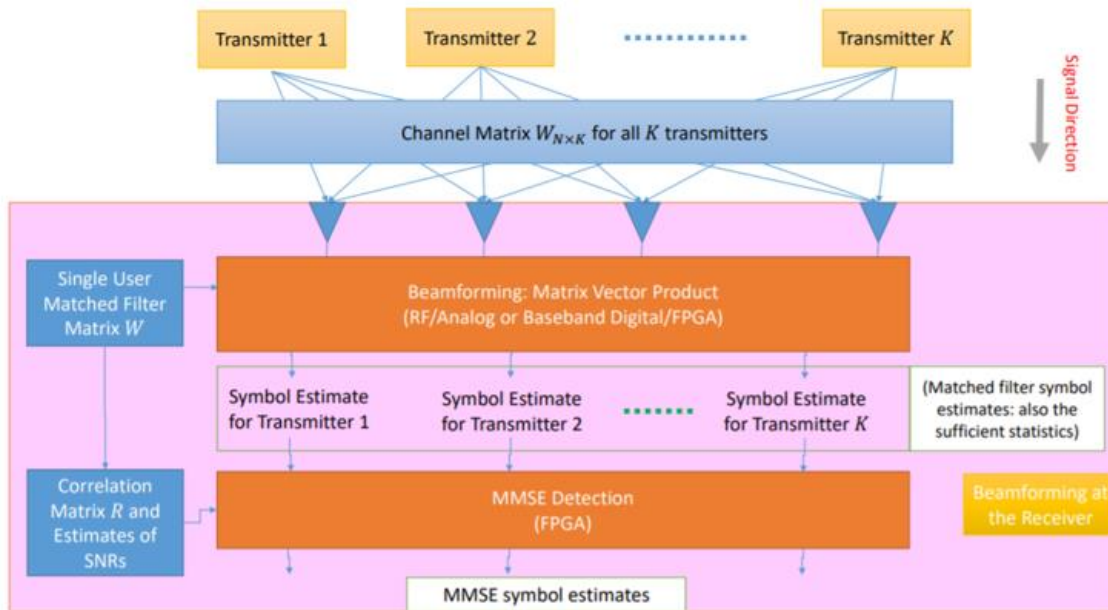


Figure 9-1 Block diagram for Beamformer

We will now look at the block diagram representations to help conceptualize these algorithms better and realize the practical implementation framework. These diagrams are drawn with a beamforming perspective, but they apply equally well to the other applications

Although these diagrams represent the system implementation architecture, the underlying operations are entirely described by linear algebra math. This math is blind to the distinction between the transmitter and the receiver. Specifically, these diagrams apply if the directions of the arrows are reversed. Instead of representing the receiver-side Beamforming, the reversed-arrow diagram illustrates the transmit-side Beamforming, also known in the literature as the transmitter precoding. Several practical considerations. The knowledge of the channel coefficients is assumed at the transmitter. The transmitter is implied to be the central unit (e.g., the base-station tower) where the information sources for different receivers are collocated. If these requirements are not met, the transmit-side precoding is usually not possible

9.4 Receiver performance Analysis

Assumes that $K = 1$ (the interference from $K - 1$ co-channel transmitters is supposed to be part of the noise vector) If all K users employ this strategy, how can we formulate the set of the decision metrics[19].

$$z = A_1 b_1 + u_1. \quad (59)$$

Let us consider a case with $K = 2$ user and BPSK modulated symbols b_1 .

For this case, R is a 2×2 matrix $R = \begin{bmatrix} \rho_{11} & \rho_{12} \\ \rho_{21} & \rho_{22} \end{bmatrix}$. Let $\rho_{12} = \rho_{21} = \rho$. Thus,

$$R = \begin{bmatrix} 1 & \rho \\ \rho & 1 \end{bmatrix}. \quad (60)$$

The receiver statistic formed by the SUMF for the two users is given as

$$\begin{bmatrix} Z_1 \\ Z_2 \end{bmatrix} = R \begin{bmatrix} A_1 & 0 \\ 0 & A_2 \end{bmatrix} \begin{bmatrix} b_1 \\ b_2 \end{bmatrix} + \begin{bmatrix} u_1 \\ u_2 \end{bmatrix} \quad (61)$$

Let us consider the receiver statistic for user 1

$$z_1 = A_1 b_1 + A_2 \rho b_2 + u_1 \quad (62)$$

Since $|\rho|$ is typically less than 1, the above occurs only if the received amplitude of User 2 is much greater than the amplitude A_1 . Practically User 1 is far from the base station compared to User 2, which is nearer. The BPSK symbol for User 1 is detected correctly if determined by whether $b_2 = 1$, and it is detected incorrectly if $b_2 = -1$.

Since b_2 takes the values of $\{-1, +1\}$ with equal probability, the error probability in the detection of b_1 becomes 0.5. . This leads to the “near-far” problem at the SUMF receiver — the interference swamps the weak user’s SUMF from the strong user even in the high SNR scenario.

The decision statistics formed by the Decorrelating detector are given as

The decision statistics formed by the Decorrelating detector are given as

$$B = Ab + R^{-1}u = Ab + v \quad (63)$$

The correlation matrix of v is written as follows

$$R_{vv} = E[vv^H] = E[R^{-1}uu^HR^{-1}] \quad (64)$$

$$R^{-1}E[uu^H]R^{-1} = R^{-1}RR^{-1} \quad (65)$$

$$\sigma^2 R^{-1} \quad (66)$$

9.5 SIC(Successive Interference Cancellations)

Consider the SUMF outputs for K = 2 users:

$$z_1 = A_1 b_1 + A_2 b_2 \rho + u_1 \quad (67)$$

$$z_2 = A_2 b_2 + A_1 b_1 \rho + u_2 \quad (68)$$

Suppose $A_2 \gg A_1$ and the “near-far” effect is not compensated by power control. With the SUMF-based reception, power control becomes necessary to avoid the near-far issue.

With the power control, the nearby user is asked to attenuate its transmission power so that the users' base station's received power is nearly identical. The system requires and implements power control. In this case, since $\rho < 1$, $A_2 \rho < A_1$, i.e., the interference

from User 1 to User 2 is small. Therefore a reasonable strategy (assuming that the symbols $\{b_k\}$ are BPSK modulated) is as follows:

Form the estimate $\hat{b}_2 = \text{sign}\{z_2\}$ using the SUMF for User 2. Subtract $\hat{A}_2 \hat{b}_2 \rho$ from z_1 to obtain $\hat{z}_1 = z_1 - \hat{A}_2 \hat{b}_2 \rho$. This assumes that an estimate \hat{A}_2 of A_2 is available. The correlation coefficient ρ has been calculated.

Form the estimate $\hat{b}_1 = \text{sign}\{\hat{z}_1\}$. If $\hat{b}_2 = b_2$ and $\hat{A}_2 = A_2$, $z_1 = A_1 b_1 + u_1$. This is the ideal BPSK input completely free of interference and (unlike the decorrelator) also free of any noise amplification

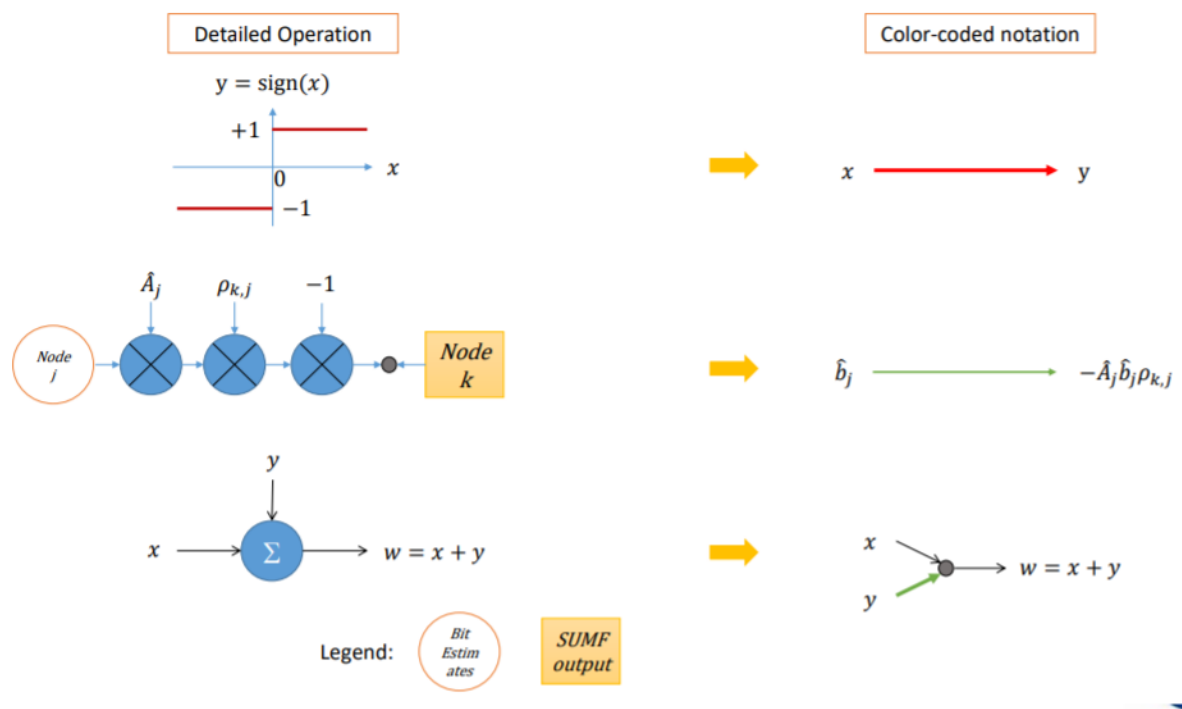


Figure 9-2 SIC

This Successive Interference Cancellation (SIC) strategy is nonlinear due to the sign operation. The interference from User 2 is eliminated, the estimate \hat{A}_2 is accurate, $A_2 > A_1$, and User 2 is demodulated first, followed by User 1 (the ordering with which different users are demodulated matters in the SIC do not want to demodulate the weak user first).

The generalization to K users case is straight -the forward extension of the prior algorithm

Estimate the amplitude estimates A_k^{\wedge} For all $k \in \{1, \dots, K\}$ and order the users based on the amplitudes and demodulate the following strongest output for K-1 users by peeling off user K contribution from SUMF output for users K-1.

$$b_k^{\wedge} = \text{sign}\{z_k - \sum_{j=k+1}^K A_j^{\wedge} B_j^{\wedge} \rho_{k,j}\} \quad (69)$$

Even in the best scenario (i.e., all the bits are decoded successfully), the SIC compensates for the interference only partially; at kth user, the interference from the Users with indices less than k (i.e., the users which are received at lower power) is not removed. This suggests a natural extension of the SIC, which is called the PIC

9.6 PIC (Parallel Interference Cancellation)

The Parallel Interference Cancellation (PIC) extends the SIC concept

Stage 1 (the SUMF):

$$b_1^{\wedge 1} = \text{sign}\{z_1\} = \text{sign}\{A_1 b_1 + A_2 b_2 \rho + u_1\} \quad (70)$$

$$b_2^{\wedge 1} = \text{sign}\{z_2\} = \text{sign}\{A_2 b_1 + A_1 b_2 \rho + u_2\} \quad (71)$$

Stage 2(the SIC on both users)

$$b_1^{\wedge 2} = \text{sign}\{z_1 - A_2^{\wedge} b_2^{\wedge 1} \rho\} \quad (72)$$

$$b_2^{\wedge 2} = \text{sign}\{z_2 - A_1^{\wedge} b_1^{\wedge 1} \rho\} \quad (73)$$

Stage 2(alternatively, iteration i)

$$\hat{b}_1^i = \text{sign}\{z_1 - A_2 \hat{b}_2^1 \rho\} \quad (74)$$

$$\hat{b}_2^i = \text{sign}\{z_1 - A_1 \hat{b}_1^1 \rho\} \quad (75)$$

The compact equation for the symbol decision formed at i th stage $\hat{b}^i = \text{sign}\{z - R \hat{b}^{i-1}\}$, where $R = R - I$ is the correlation matrix with the diagonal terms zeroed out.

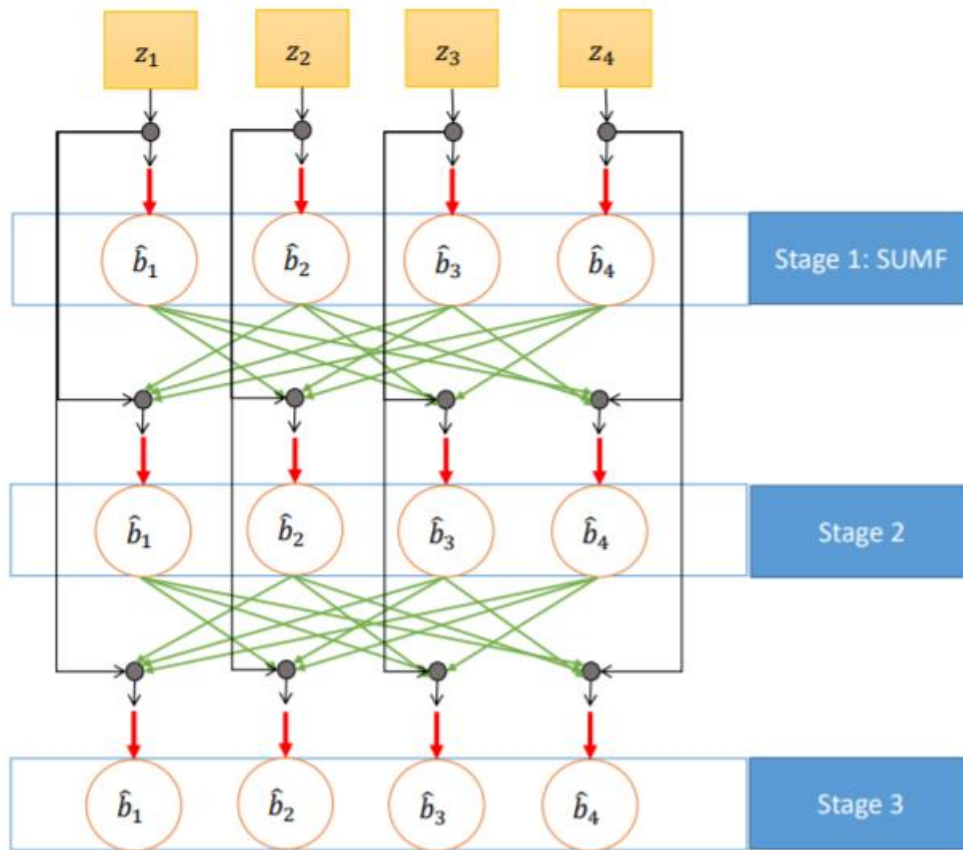


Figure 9-3 PIC

A limitation of the SIC is that the interference from the weaker users is not removed in the demodulation of the k th user. The PIC attempts to remove the interference entirely, but it can underperform if the weak user's SUMF output significantly

interferes with the stronger users. The algorithm that we consider next, called the Decision Feedback IC, solves this problem using Cholesky Factorization of the correlation matrix R . The name decision feedback is due to the legacy from the earlier research on canceling the echos in telephone landline connections. The SIC and the PIC also are the decision feedback schemes — the scheme described next performs the decision feedback in a manner slightly different from that of the SIC

9.7 Interference Cancellation by Decision Feedback

Noise whitening Transformation: By Cholesky factorization of $R=F^H F$. By multiplying the SUMF output vector $z= RAb+\sigma u$ with $F^{-H} = (F^H)^{-1}$

$$\hat{z}=F^{-H} z = F^{-H} F^H F A b + F^{-H} u \quad (76)$$

$$=F A b + \hat{u} \quad (77)$$

Here, F is a lower-triangular matrix whose diagonal elements are non-negative

The DF algorithm is conceptually identical to SIC, but correlation coefficients $\rho_{i,j}$ are replaced by $f_{i,j}$. And the triangular nature of the F matrix implies complete interference cancellation.

Estimate the amplitude estimates $A_k \hat{}$ for all $k \in \{1, \dots, K\}$ and order the users based on the amplitudes and demodulate the following strongest user by simply using whitened SUMF output

$b_1 \hat{=} \text{sign}\{z_1 \hat{}$. Demodulate the following more robust user simply by peeling off user one contribution from SUMF output for users 1.

$$b_2 \hat{=} \text{sign}\{z_k \hat{ - A_1 \hat{ B_1 \hat{ f_{2,1}}}} \quad (78)$$

$$b_k \hat{=} \text{sign}\{z_k \hat{ - \sum_{j=k+1}^k A_j \hat{ B_j \hat{ f_{k,j}}}} \quad (79)$$

Even in the best scenario (i.e., all the bits are decoded successfully), the SIC compensates for the interference only partially; at k th user, the interference from the Users with indices less than k (i.e., the users which are received at lower power) is not removed. This suggests a natural extension of the SIC, which is called the PIC

Estimation of A_k is not addressed: this is an area of research. To study the best performance these algorithms can deliver, A_k can be assumed to be known perfectly. The concept and the mathematics are more straightforward — especially the SIC and the PIC schemes require only the multiplications, subtractions, and sign operations (matrix algebra is not needed, unlike the linear schemes), the linear algebra concepts are not required either. These schemes suffer from the problem of error propagation — if a symbol for a user is estimated in error, it can worsen (instead of reducing) the interference seen by the other users and their symbols, in turn, be detected erroneously. Possible remedies. Replace the sign nonlinearity with a softer version, e.g., hyperbolic tangent function, or a thresholded nonlinearity (that ignores the soft symbol values close to the decision boundary)

9.8 Simulation Result

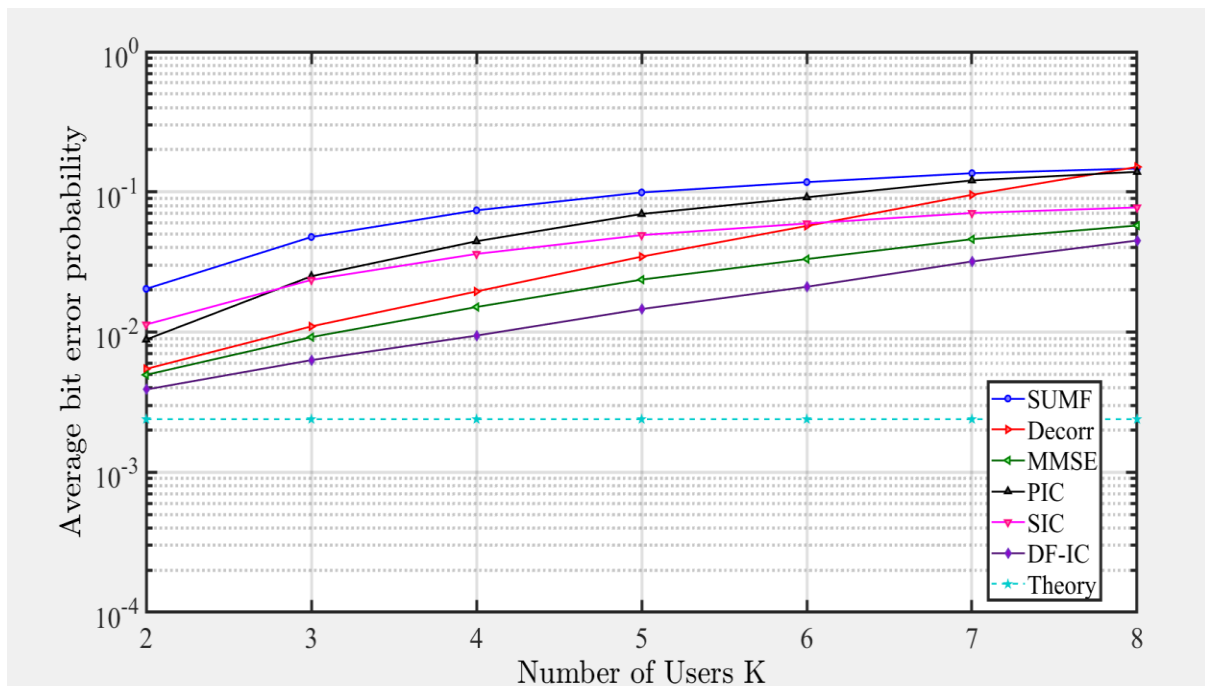


Figure 9-4 Plot for Avg. Bit Error Rate and Number of User K

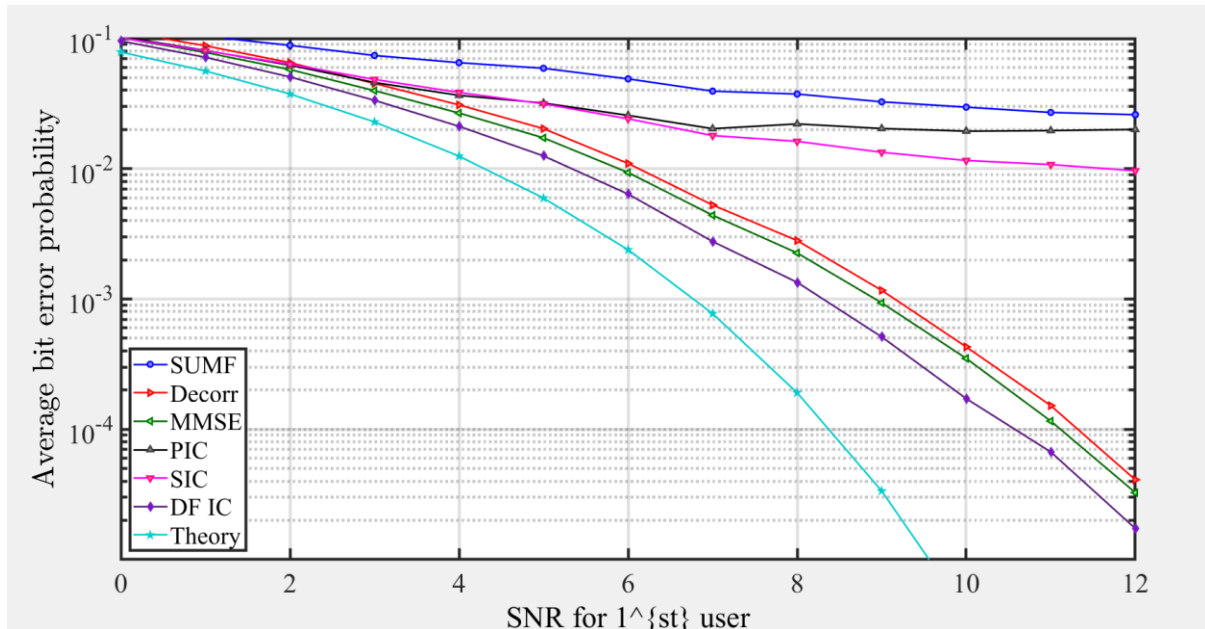


Figure 9-5 Plot for avg Bit Error Rate and SNR for user 1

The performance of DF-IC is close to the theoretical error performance, as we can see from figure 9-4. MMSE and decorrelating receivers have similar error performances. As several users increase, the performance of the nonlinear method is better than the

linear one in error performance. In a linear family, MMSE performs the best. In a nonlinear family, DF-IC performs the best.

10 Conclusion and Scope of future work

10.1 Conclusion

In this thesis, the theory of Array Signal Processing for ULA is reviewed for the direction of the arrival estimation problem. We have discussed spectral analysis for solving the direction-finding problem. Conventional beamforming methods and the MVDR method have been discussed. The performance and limitations of these algorithms have been reviewed by providing MATLAB simulations. The MUSIC method, a subspace-based algorithm, has also been addressed in this Thesis. We review the performance of MUSIC using MATLAB simulations and compare its resolution with non-parametric methods discussed earlier. The limitations of MUSIC are also discussed later.

Further Expectation-Maximization has also been simulated in MATLAB. It is also inferred that the direction of arrival estimation can be done with better accuracy if the SNR is adequately high. Also, MMSE for MVDR and MUSIC has been simulated in MATLAB.

Array processing enables one to perform spatial filtering of signals thanks to additional degrees of freedom. Adaptive Beamforming, possibly with reduced-rank transformations, allows one to achieve high SINR with a fast convergence rate in adverse conditions (interference, noise). Robustness issues are of utmost importance in practical systems and should be given careful attention. Non-parametric direction-finding methods are simple and robust but may suffer from a lack of resolution. Parametric methods offer high resolution, often at the price of degraded robustness.

We implement array factor and radiation polar plots of both Planar and Circular Array in the next stage. We also researched and tried to implement DOA estimation in UCA and UPA USING MUSIC.

Next, we studied various interference cancellation techniques like SUMF, MMSE, SIC, PIC, DF-IC, and comparative study.

10.2 Scope of Future Research

Currently, we did a deep study of linear or one dimension of uniform linear array setup has also been simulated we tried to research on two-dimension arrays and plotted its array factor and doa estimation using MUSIC. The two-dimension investigation is more following the real-time environments where both elevation and azimuth angles are needed. Also, the circular array is the main requirement for the GNSS satellite communication system. Further research will be on these array geometry and simulation algorithms for DOA estimation for these geometries. So we tried to implement a circular array radiation pattern and did its doa estimation using MUSIC, CAPON.

Further research will be focussed on the Mitigation of Jammers and interferers for this array. Therefore, a faster algorithm for solving optimization functions is worthy of further research. The power of the desired signal from GNSS is much weaker than the power of the interferences. Estimating the DOA of the interferences will help first isolate the jamming/interfering signals, and then we can estimate our desired DOA. Hence, an extensive study of various DOA estimation techniques, MUSIC, ESPRIT, Expectation-Maximization, is required for circular array and study null depth. Another point of research will be the null depth. We explored various interference

cancellation techniques like SUMF, MMSE, SIC, PIC, DF-IC, and their comparative study.

11 REFERENCES

- [1] "Degree of Arrival Estimation for Uniform Planar Array.pdf."
- [2] H. Krim and M. Viberg, "Two decades of array signal processing research: The parametric approach," *IEEE Signal Process. Mag.*, vol. 13, no. 4, pp. 67–94, 1996, DOI: 10.1109/79.526899.
- [3] S. Shirvani-Moghaddam and F. Akbari, "A novel ULA-based geometry for improving AOA estimation," *EURASIP J. Adv. Signal Process.*, vol. 2011, no. 1, pp. 1–11, 2011, DOI: 10.1186/1687-6180-2011-39.
- [4] O. Besson, "Introduction to Array Processing."
- [5] Y. Vasavada, "CT-509 Next Generation Wireless Communication Systems," no. August 2020.
- [6] C. A. Balanis, "Antenna Theory: A Review," *Proc. IEEE*, vol. 80, no. 1, 1992, DOI: 10.1109/5.119564.
- [7] S. N. Shahab, A. R. Zainun, N. H. Noordin, and S. S. Balasim, "Assessment of MVDR Adaptive Beamforming algorithm in uniform linear arrays, uniform rectangular arrays, and uniform circular arrays configurations," *ARPJ. Eng. Appl. Sci.*, vol. 11, no. 6, pp. 3911–3917, 2016.
- [8] A. Dalli, L. Zenkouar, E. L. F. Adiba, M. Habibi, and S. Bri, "Circular Array with Central Element for Smart Antenna," vol. 3, no. 3, pp. 86–95, 2013, DOI: 10.5923/j.eee.20130303.02.
- [9] B. D. Van Veen and K. M. Buckley, "Beamforming: A Versatile Approach to Spatial Filtering," *IEEE ASSP Mag.*, vol. 5, no. 2, pp. 4–24, 1988, DOI: 10.1109/53.665.
- [10] F. Belloni, A. Richter, and V. Koivunen, "Extension of root-MUSIC to non-ULA Array Configurations," pp. 897–900, 2006.

- [11] F. Belloni and V. Koivunen, "Unitary root-music technique for uniform circular array," pp. 451–454.
- [12] A. M. Montaser, K. R. Mahmoud, A. B. Abdel-rahman, H. A. E. Senior, and M. Ieee, "CIRCULAR, HEXAGONAL AND OCTAGONAL ARRAY GEOMETRIES FOR SMART ANTENNA SYSTEMS USING HYBRID CFO-HC ALGORITHM," vol. 40, no. 6, pp. 1715–1732, 2012.
- [13] S. Sekizawa, "Estimation of Arrival Directions Using MUSIC Algorithm with a PlanarArray," vol. 2, pp. 555–559.
- [14] "lecture3_CT509_YASH_VASAVADA.pdf."
- [15] J. G. Andrews, "Interference cancellation for cellular systems: A contemporary overview," *IEEE Wirel. Commun.*, vol. 12, no. 2, pp. 19–29, 2005, DOI: 10.1109/MWC.2005.1421925.
- [16] N. K. Raj Kamala J Silva Lorraine, "Comparative Analysis of Various Beamforming Techniques for Interference Cancellation in GPS receivers," vol. 7.
- [17] N. Y. Wang and P. Agathoklis, "A new high-resolution-and-capacity DOA estimation technique based on subarray beamforming," *Conf. Rec. - Asilomar Conf. Signals, Syst. Comput.*, vol. 2, no. 9, pp. 2345–2349, 2004, DOI: 10.1109/acssc.2004.1399588.
- [18] R. De Miguel and R. R. Müller, "Vector precoding for a single-user MIMO channel: Matched filter vs. distributed antenna detection," *2008 1st Int. Symp. Appl. Sci. Biomed. Commun. Technol. ISABEL 2008*, 2008, DOI: 10.1109/ISABEL.2008.4712589.
- [19] A. Sayeed and J. Brady, "Beamspace MIMO for high-dimensional multiuser communication at millimeter-wave frequencies," in *GLOBECOM - IEEE Global Telecommunications Conference*, 2013, pp. 3679–3684, DOI:

12 Appendix

12.1 MATLAB CODES

hold on

```
set(0,'DefaultAxesLineWidth', 2.5);
set(0,'DefaultLineLineWidth', 3.0);
set(0,'DefaultAxesFontName','times')
set(0,'DefaultAxescolor','w')
set(0,'DefaultTextcolor','k')
set(0,'DefaultTextFontName','times')
set(0,'DefaultAxesFontSize',24)
set(0,'DefaultTextFontSize',20)
set(0,'DefaultTextInterpreter','Latex')
%to setthe default value for standard plots;
clc;
close all;
N=12;
n=0:N-1;
K=3;
aaq = [30 0 5];
paaq = 10.^(aaq/10);
```

```

% K = 10;

% N=20;

M=1024;

% theta = [-50 -35 -20 -10 0 10 20 35 50 70];

% theta = [37.3708 26.8868 -52.6009 65.4090 41.6733];

theta = [-20 0 20];

% theta =[-8.7442 59.4604 51.0955 87.9849 -88.8242]

% ak = ones(K,1);

a_k = paaq';

a_k = ones(K,1);

SNR_dB=20;gamma=10^(SNR_dB/10);sigma=1/sqrt(gamma);

M=1024;t=0; do = 0:0.1:10;do(1)=[];

% di = -10:0.1:0;di(end)=[];

% for ii =1:length(do)

% theta=[-di(ii) 0 do(ii)];

theta=theta.*(pi/180);

f=sin(theta)/2;

phi_k=2*pi*rand(K,1)-pi;f=f(:);

%% PSD

xn_k = a_k.*exp(1j*2*pi*theta').*exp(1j*2*pi*f*(0:N-1));

for kk=1:N

xnk=xn_k(:,kk);

```

```

R=xnk*xnk';
t=t+R;
f_k=f.';
W=exp(-1j*2*pi*n'*f_k);
u = sigma*randn(N,1)+1j*randn(N,1);
xn = W*xnk+u;
end
R_ss=t/N;
Rss = diag(a_k.^2);
Rxx=W*R_ss*W'+sigma^2*eye(N);
fo = linspace(-0.5,0.5,M);
r = fftshift(fft(Rxx(1,:),M));
r1 = abs(r);
r2 = 10*log10(r1/max(r1));
plot(fo,(r2),'linewidth',2);
hold on;
xlabel('$\mathrm{\sim Distance\sim along\sim the\sim depth\{(mm)\}}$','fontsize',24,'fontweight','b','color','k','fontname','Times New Roman','interpreter','latex');
ylabel('$\mathrm{\sim Stress\}\mathrm{\{(MPa)\}}$','fontsize',24,'fontweight','b','color','k','fontname','Times New Roman','interpreter','latex');
legend({'S11','S22','S33','SMises'});

```

```

axis square
set(gca,'box','on');
set(gca,'XMinorTick','on')
set(gca,'YMinorTick','on')
set(gca,'TickLength',[0.02 0.04]);
%legend boxoff
% legend('PSD')
% %
% [pk,lc] = findpeaks(r2,fo);
%
% hold on
% plot(lc,pk,'x')
grid on;
% %
xlabel(' Normalised frequency f');
ylabel('PSD in db');
% title('Matched-filter (DFT) based power spectral density (PSD)
estimation')

%% MUSIC
[Q,D]=eig(Rxx);
k=sum(sum(round(D)~=0));
K1 = N-k;

```

```

V = Q(:,[k+1:end]);
W1 = exp(-1j*2*pi*n*fo);
for i = 1:length(fo)
PsePSD(i) = 1/((W1(:,i)')*(V*V')*W1(:,i)));
end

Pmusic=10*log10(abs(PsePSD)/max(abs(PsePSD)));           %Spatial
spectrum function plot(fo,Pmusic,'linewidth',2) ;
plot(fo,(Pmusic),'linewidth',2);
hold on;
% legend('MUSIC')
grid on;
xlabel(' Normalised frequency f');
ylabel('PSD in db');
% [pk1,lc_music] = findpeaks(Pmusic,fo);
% lc=lc(1:11-1);
% grid on;
% mse_mf = (f_k-lc_music).^2;
%% ESPRIT
[E, D] = eig(0.5*(Rxx + Rxx'), 'vector');
% [E, D] = eig(Rxx);
Es = E(:,end-K+1:end);ds=1;
Es1 = Es(1:end - ds,:);

```



```

Es2 = Es(ds + 1:end,:);
C = [Es1 Es2];
C = C'*C;
C = 0.5*(C + C');
[V, l] = eig(C, 'vector');
[~, idx] = sort(real(l), 'descend');
V = V(:,idx);
V12 = V(1:K,K + 1:end);
V22 = V(K+1:end,K+1:end);
Phi = -V12/V22;
zz = eig(Phi);
ang = -asin(angle(zz)/pi)*180/pi
%% MVDR
W1 = exp(-1j*2*pi*n'*fo);
for i = 1:M
P_MVDR(i) = 1/(W1(:,i)'*inv(Rxx)*W1(:,i));
end
Pmvdr=10*log10(abs(P_MVDR)/max(abs(P_MVDR)));      %Spatial
spectrum function
hold on;
plot(fo,(Pmvdr),'linewidth',2);
hold on;
% legend('MVDR')

```

```

xlabel(' Normalised frequency f');
ylabel('PSD in db');
% %% MF
y = xn*W1;
y_mf=10*log10(abs(y)/max(abs(y)));
plot(fo,(y_mf),'linewidth',2);hold on;
% % legend('MF')
%% Window Wrong
% wc = kaiser(N,2.4);
% xn = xn.*wc;
% y = xn*W1;
% y_win=10*log10(abs(y)/max(abs(y)));
% plot(fo,(y_win),'linewidth',2);hold on;
%% EM
W1 = exp(-1j*2*pi*n*fo);%Reference filter bank
%Random initialization of Rzz
rnf = rand(M,1);
Rzz = diag(rnf.^2);
Xn = W*xn_k+sigma^2*eye(N);
% Rzz = eye(M);
for i = 1:20
Rxx1 = W1*Rzz*W1';
Rxx1 = Rxx1/N;

```

```

Rxx_inv = inv(Rxx1);

for mm = 1:M

w_m = W1(:,mm);

w_mvdr = Rxx_inv*w_m/(w_m'*Rxx_inv*w_m);

y_em = w_mvdr'*Xn;

for aa = 1:12

y_em(:,aa) = w_mvdr'*Xn(:,aa);

end

Rzz(mm,mm) = y_em*y_em';

end

end

P_em = abs(diag(Rzz));

P_EM=10*log10((P_em)/max((P_em)));

plot(fo,((P_EM)), 'linewidth',2);

hold on;

plot(f_k,-75,'ro','markerfacecolor','r')

grid on;

% legend('EM')

xlabel(' Normalised frequency f');

ylabel('PSD in db');

% plot(f_k,'ro')

```

```
legend({'PSD','MUSIC','MVDR','MF','EM'})
```